A STUDY OF THE EFFECTS OF VIBRATIONS ON RESOLUTION AND ACUTANCE OF IMAGERY FROM THE ZEISS RMK AR 15/23 CAMERA

A Thesis

Presented in Partial Fulfillment of the Requirements
for the Degree Master of Science

by

David Francis Maune, B.S.

The Ohio State University
1970

Approved by

Adviser
Department of Geodetic Science

ACKNOWLEDGMENT

The author wishes to acknowledge the valuable assistance provided by the following associates:

Dr. Sanjib K. Ghosh, Associate Professor, Department of Geodetic Science, The Ohio State University, who provided overall guidance and valuable assistance in the accomplishment of this project.

Dr. J. K. Davidson, Assistant Professor, Department of Mechanical Engineering, The Ohio State University, who assisted with the equation of motion phase of resolution prediction.

Mr. Don Groening, Avionics Laboratory, Wright-Patterson Air Force Base, Ohio, who assisted in planning and effecting the data acquisition phase of the project.

Mr. Paavo Loosberg, Data Corporation, who made invaluable recommendations and assisted in the camera testing and film processing phases of the project.

Mr. Elwood Dornbusch, Data Corporation, who assisted with the targeting and camera vibration phases of the project.

Mr. C. W. Anderson, Avionics Laboratory, Wright-Patterson Air Force Base, Ohio, who assisted with the transducer assembly and vibration recording portion of the project.

Special thanks are due to the entire Photo-Optical Section of the Avionics Laboratory, Wright-Patterson Air Force Base, Ohio, who generously provided equipment, supplies and technical assistance necessary to complete this work.

The author also expresses his appreciation to his fellow students who assisted with computer programming, resolution determination, drafting etc., as well as to Mrs. Guytanna Swisher for her assistance in the preparation of the report.

TABLE OF CONTENTS

I. INTRODUCTION

I.A Aerial Camera Mounting Methods

There are several ways in which an aerial camera or aerial camera system can be mounted in an aircraft/spacecraft.

The simplest method is to rigidly bolt the camera onto the airframe. The camera body can now be considered as an extension of the airframe, i.e., experiencing the same motions and vibrations as the aircraft/spacecraft. In some cases, the vibration spectrum anticipated may be sufficiently small to permit this type of mounting; however, the effects of landing shocks upon the camera may cause detrimental internal movement of the camera system components. For this reason, the method of rigid mounting is rarely used.

When it is necessary to achieve the highest resolution possible, the best camera mounting system available is that which provides a stabilized platform for the camera system to operate from. Using gyroscopic references and electronic controls, these platforms can keep a camera relatively motionless in spite of very severe external perturbations and vibrations. In addition to providing the best steadiness, stabilized platforms also provide a highly accurate vertical direction/attitude to which the camera may be precisely referenced. While the gyroscopically stabilized platform is the best available means for mounting aerial cameras, it also is the heaviest, requires the most space and is the most costly.

In between the two extremes of a rigid mounting and a stabilized platform, is the method using vibration isolators or spring type devices. Although the vibration isolators afford no compensation for aircraft roll, pitch and yaw motions, they do offer excellent isolation against airframe vibrations as well as providing shock protection for the camera. For this reason, and because of its simplicity and inexpensiveness, the vibration isolator is the mounting device most generally used. As a consequence, however, users tend to accept resultant imagery as the best available under the circumstances, without questioning that the results achieved might not reflect the full capability of the camera system being used. It would be a safe bet that someone, desiring improved resolution, would try to obtain it by using a finer grained film in the same camera system. Yet it might be the camera system itself and not the film, that is causing poorer quality parameters than desired. More specifically, the dynamic environment of the camera system may be the culprit in the whole photographic process.

I.B Dynamic Environment

The dynamic component of an aerial photographic system consists of two interacting sub-components:

The internal dynamic system of a camera including the motors, shutter, film advance mechanism and all other moving parts which establish a dynamic environment through the operation of the camera alone.

The external dynamic system including vibrations from the camera stabilization system (mount), dynamic response from the aircraft/spacecraft caused by engine vibrations, air turbulence etc., and all other factors which cause the camera to receive external excitation.

The fact that image motion causes degradation of photographic image quality is mentioned in many photogrammetric references. That portion of image motion caused by vibrations, however, is literally neglected in textbooks but has been the subject of several special studies, some of which are referenced in this report. However, there is a need for laboratory controlled dynamic tests of a complete camera system in its operational mode to supplement the mathematical approaches and those actual dynamic tests which project the results of limited laboratory conditions to those conditions which would be experienced in a normal operational mode.

I.C Image Quality Parameters

If image quality degradation is to be studied, one must first decide which image quality parameters should be used. In chapter 23 of reference [1], James and Mees discuss the many subjective and objective parameters used and the dozens of studies devoted to the subject.

It is generally agreed that resolving power is one valid parameter for judging image quality or definition, and a relatively objective determination of resolution is easily obtained. (This paper will normally refer to resolving power as a capability, and to resolution as the actual result. In other words, although a camera lens, film etc. indicates a certain resolving power capability, vibrations could cause poorer actual resolution values.)

The modulation transfer function (MTF) is gaining popularity at this time; however, its value is debatable, and it requires special instrumentation that was not readily available locally.

Sharpness is an image quality parameter that everyone appreciates when studying a photograph, but sharpness is basically a subjective term. Acutance, nevertheless, is advertised as the objective correlate of sharpness, i.e., acutance is supposed to determine, without human prejudice, the relative sharpness of image edges. Except for a microdensitometer and auxiliary equipment, all of which is locally available, no special targeting or instrumentation is required beyond that for resolution determinations.

Therefore, it was decided that the image quality parameters to be studied would be resolution and acutance.

I.D Objectives

The objectives of this study are the following:

1. To determine the static resolution and acutance capabilities of a camera system for subsequent comparison with these parameters when the camera system is subjected to internal and external dynamic loading.

2. To isolate the internal dynamic components of a camera system, and to determine what image degradation occurs as a result of these individual and combined components.

3. To apply, to the camera system, laboratory controlled and measured steady state vibrations over the frequency and amplitude range of normal expectancy for camera systems; to study image quality degradation resulting from this external dynamic loading.

4. To assess the criticality of vibrations in general on image quality, and to make recommendations for improving camera system performance, if possible.

II. VIBRATION ISOLATION

Translational and rotational vibrations of a camera during the exposure period result in a relative motion of the image over the film with a consequent loss of image quality. Fish [2], however, describes how pure translational motion of the camera has the same effect on the image as if the camera were held still and the ground moved by the same amount. With current camera systems it is obvious that camera translations of a fraction of an inch can easily be tolerated since aerial cameras cannot detect such small movements of the object space.

Rotation of the aircraft/spacecraft or the camera system about its x (longitudinal), y (lateral) or z (vertical) axes during the exposure period, however, has considerable consequences. This rocking type of motion causes a notable image shift which would affect any parameter used to judge image quality.

One might logically ask how rotational vibrations become involved when the input vibrations are basically up and down, back and forth, or various combinations of translational vibrations. The answer to this question is simple. The solution to the problem is not so simple.

The answer can best be explained with the help of the adjacent diagram. Assume the elastic center of the vibration isolation system of an aerial camera is at the point marked e.c., and assume the center of gravity of the camera is at the point marked c.g.

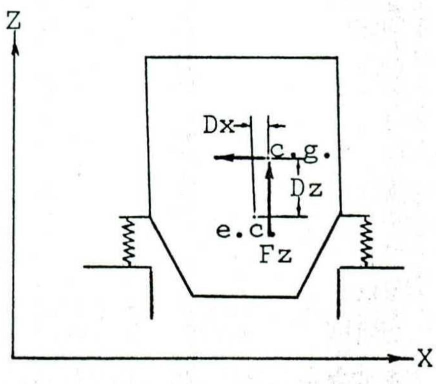

The center of gravity is displaced from the elastic center by Dx and Dz as shown, and also by Dy not shown, which is directed perpendicular to the plane of the paper. A vertical vibration, with inherent acceleration, will effectively act upon the mass concentrated at c.g. and will create the force Fz, where Fz equals the camera mass (effectively concentrated at the center of gravity) multiplied by the vibration acceleration in the Z-direction. Similarly, a vibration in the X-direction will have an acceleration in the X-direction which acts on the camera mass at the center of gravity and creates the force Fx in the X-direction. Not shown is a force Fy, directed perpendicular to the plane of the paper, which results from the acceleration of a Y-direction vibration acting on the mass at the center of gravity.

In the XZ plane of motion, the force Fx acts on moment arm Dz to form a couple or torque about the elastic center of the isolation system. Similarly, Fz acts on moment arm Dx to form another couple or torque about the elastic center. These coupling forces are continuously changing in magnitude and direction because the acceleration components vary sinusoidally and are independent from each other in the X and Z directions. Although both forces Fx and Fz are shown in the case where they each produce a counterclockwise torque, it is equally possible that they combine to form a clockwise torque, or opposing torques which partially cancel each other. Obviously, the greatest amount of rocking motion is obtained when these torques reinforce each other in the same direction.

In the YZ plane of motion (not shown), the force Fy acts on the same moment arm Dz as before, and the same force Fz acts on moment arm

Dy. These forces acting on moment arms produce couples or torques in the YZ plane of motion and cause a rocking motion in that plane.

In the XY plane of motion, Fx acts on moment arm Dy and Fy acts on moment arm Dx. However, the vibration isolators are resistant to (shear type) coupling forces in the XY plane and effectively allow movements only in the vertical directions. Thus, any XY plane rocking motion (swing/kappa type oscillation) is negligible. For this reason, most vibration isolated camera systems are considered to have three primary degrees of freedom, i.e., since the isolators generally allow movements in the Z (up/down) direction only, the three principal motions the camera system can have are (1) Z-direction translation, (2) YZ plane rotation about the X-axis, and (3) XZ plane rotation about the Y-axis. The three secondary degrees of freedom, which are normally ignored in developing equations of motion, are (1) X-direction translation, (2) Y-direction translation, and (3) XY plane rotation about the Z-axis.

For detailed explanations of these principles, the reader is referred to Crede [3], for an analysis of rotatory motions caused by internal vibrations, and to Crafton [4], for an analysis of rotatory motions caused by external vibrations. In addition to these textbooks on shock and vibrations, Casper [5] has prepared an interesting paper which deals specifically with aerial cameras and the theoretical development of motions caused by vibrations acting on an unbalanced camera system.

The primary reasons for camera unbalance are the following:

1. The center of gravity of a camera lies in a horizontal plane which normally contains important camera components for which accessability is mandatory. Thus the camera mount with isolators cannot surround

the camera at the level of this horizontal plane and is lowered for convenience.

2. A mount with three isolators is best for leveling purposes, and most cameras are basically rectangular in cross section since the photograph format is rectangular. Thus the three point suspension of a rectangular object presents an added design problem in balancing the system.

3. Partly because of the previous problem and partly because of uneven weight distribution of camera components, the three isolators normally carry uneven weights.

4. There is considerable difficulty in matching spring and damping constants for the differently loaded isolators, required to prevent additional system unbalance.

5. There is always uncertainty in the location of the isolation system elastic center.

6. There is some uncertainty in the location of the center of gravity caused by manufacturing tolerances.

7. Film transfer from storage spool to take-up spool theoretically requires compensation as the center of gravity shifts accordingly.

All of the above considerations are fundamental to the design of a balanced camera system. In addition, there is the critical problem of selecting vibration isolators with the proper spring and damping constants, natural vibration frequencies etc. to provide optimum damping of all anticipated vibrations. Improperly selected vibration isolators may amplify rather than attenuate undesired motions imparted to the camera. As a result photographic quality can be unnecessarily degraded.

III. DATA ACQUISITION

III.A Instrumentation

III.A.1 Camera System

Because of its availability, and the fact that it is representative of the modern commercial aerial camera, the Zeiss RMK AR 15/23 camera, belonging to The Ohio State University Department of Geodetic Science, was used for the test. An outline of the camera system with center of gravity positions is shown at Figure 1. In this figure, CG_L is the position of the center of gravity with a 400 foot roll of film on the left spool; CG_R is the position of the center of gravity with the film on the right spool. CG indicates the central position with half of the film on either spool, and CG_0 is the position with no film.

Characteristic curves of the Vibrachoc vibration isolators used are shown at Figure 2. Vibrachoc isolators are a French product designed specifically for the protection of electronic apparatus against vibrations and shocks aboard modern aircraft, remote control machinery and similar equipment. Their operational efficiency is allegedly not influenced by variations of temperature, humidity, dust, oil, water or ice conditions, air-density, ozone, mildew or micro-organisms. All information on the Vibrachoc isolators was extracted from reference [16], a Vibrachoc publication provided to the author by the Zeiss organization.

The Vibrachoc is an all metal isolator consisting of a helical spring filled with a knitted cushion of rustless steel wire coils, similar in some respects to steel wool. It has the combined effect of a spring - dashpot system. The spring has a weak natural frequency for effective vibration isolation, and the auxiliary cushion acts during temporary overloading and serves as an elastic protection buffer against shocks.

As is shown in Figure 2, the isolators are non-linear, giving them a large load tolerance with limited distortion. Appendix D will include a more thorough analysis of these curves.

III.A.2 Vibration Simulator

The camera system was mounted in an aircraft vibration simulator (Figure 3) at the Air Force Avionics Laboratory, Wright-Patterson Air Force Base, Ohio. The simulator was equipped with MB Electronics Model T-195 Vibration Test Equipment capable of producing steady state sinusoidal type vibrations of variable amplitude with a frequency range of 5 through 500 cps. This vibration capability matched the photographic aircraft vibration spectrum listed in Procedure XII of MIL-E-5272, a U.S. government publication covering various environmental conditions for many types of aircraft.

III.A.3 Targeting

Two interchangeable USAF resolving power test targets were used, one of 1000:1 and one of 6:1 contrasts, referred to herein, respectively, as the high and low contrast targets. The design of the high contrast target is shown at Appendix A, which also lists the calculations involved in determining resolution values. The low contrast target has the same design as the high contrast target, except that the background is grey instead of white. The large black rectangle provides edges for scanning purposes. It is obvious that this target affords the opportunity to scan edges and measure resolution values in both the x and y directions.

Target illumination was provided by a 500 watt xenon lamp in a twelve inch integrating sphere (Figure 4). At the exit of the integrating sphere was located a slide box for the insertion of neutral density filters as required for illumination attenuation. Next, in order of positioning, was a modified Rapidyne shutter from a KA2 twelve inch camera. Although limited in speed to 1/350th of a second and slower, this shutter provided a capability for external exposure control. This shutter was aligned with the objective end of an 80 inch F8 collimator. After leaving the collimator, light rays from the target were reflected off of a mirror positioned at a 45 degree angle so as to reflect the parallel rays from the collimator up through the bottom of the aircraft vibration simulator into the camera where the target image was positioned at the center reseau cross of the format.

III.A.4 Vibration Measurement

The camera was fitted with three accelerometers and three M.B. Electronics Model 122 vibration pick-up transducers, mounted in a specially built bracket so that mutually perpendicular translational vibration measurements could be taken in the x, y and z directions. This assembly (Figure 5) will be referred to as the transducer assembly - a transducer being a device which converts shock or vibratory motion into an electric signal that is proportional to the parameter of the experienced motion. These transducers were then connected to a power supply, an amplifier and a Honeywell Oscillograph (Figure 6) which plotted the vibration characteristics received at the camera along the three major axes. The amplifier contained discrete dial settings for gain control required in adjusting amplitudes of recorded values. The transducers, oscillograph and gain control settings had previously been jointly calibrated for direct conversion of recorded amplitudes into accelerations and velocities of the measured vibrations. The chart speed could likewise be adjusted up to a maximum of 40 inches/second, which was fast enough to be able to count recorded vibration frequencies up to and including 500 cps.

III.B. Test Procedure

III.B.1 Film Preparation Phase

The film magazine was loaded with Kodak Panatomic X SO-136 film. This fine grained mapping film, with characteristics as explained in Appendix B (an extract from Kodak Publication No. M-118-N), was selected so that the camera system, and not the film itself, would be the limiting factor in the resolution and acutance determinations.

A series of test exposures were made, and it was decided to conduct the test using f/5.6 aperture with exposure times of 1/200 and 1/500 second, with 0.3 neutral density filter light attenuation required for the 1/200 second exposures.

In addition to making all subsequent exposures at either of these two exposure times, each film strip was exposed in an Eastman Intensity Scale Sensitometer Automatic Type IB, Model IV, to a density step wedge for subsequent density calibration.

In deciding on the number of exposures to be made under each test condition it is necessary to analyze just what effect a vibration has during an exposure. If one considers the common steady state type of vibration as a rotating vector, plotting the amplitude of vibration against time produces the common sine curve where the sine wave period is equal to the inverse of the vibration frequency. Considering a 5 cps vibration, it is obvious that the time period of the sine wave is 1/5th second, but the exposure is made over only a small fraction, 1/200th or 1/500th second, of that vibration period. If the exposure is made when the vibration phase angle is near $\pi/2$ or $3\pi/2$, the cosine of the vibration, which represents the velocity, is near zero; thus there will be practically no image motion during the exposure. However, if the exposure is taken when the vibration phase angle is near 0 or π, the velocity is near its maximum value and maximum image motion should result. This would be the condition we are interested in if a single vibration phase angle created a maximum rotatory motion of the camera. However, as was shown in section II, maximum image motion would be obtained in the XZ plane, for example, when the vibration accelerations in both x and z directions cause maximum torques in the same direction (clockwise or counterclockwise) about the center of gravity. It is this latter condition that we are interested in.

Although we have no way of assuring that an exposure is made at the time of maximum image motion, we can apply the laws of statistics to determine the probability that at least one of many photos is taken within a vibration range near the maximum image velocity. The calculations of Appendix C indicate that one photo of twenty should be taken within 90 - 100 % of maximum vibration velocity with a probability of about 94% in the x-direction and with a probability of about 97% in the y-direction. Therefore, by selecting the poorest resolved photo of 20 taken in a series under identical conditions, it is quite probable that this photo was taken very near to or included that portion of the vibration cycle where image degradation should be most severe. Since the same general reasoning can be applied to all photographs taken when the exposure time is less than a vibration period, twenty exposures were made of each external vibration test condition using vibration frequencies less than 200 cps. However, since full double amplitude vibration is assured for all excitation frequencies equal to or exceeding 500 cps, only three exposures were made under those conditions to avoid what was thought to be wasteful redundancy. In the case of internal vibrations, when it was not positive that vibration frequencies exceeded 500 cps, it was decided to take five exposures under each test condition to provide a little better margin of safety.

III.B.2 Internal Vibration Phase

During the internal vibration phase of the test it was desired to see what vibration effect the various internal motors of the camera system would have on resolution and acutance. The experiment was conducted in four steps as follows: In step 1, the static situation, no motors were run internally. In step 2, only the vacuum motor was run internally. In step 3, only the main motor (which operates the shutter and film advance system) was run internally, and in step 4, both internal motors were run in the normal operational mode, without external excitation. In steps 1 and 2, 1/200 second exposures were made with the external shutter, and the film was advanced by hand between exposures; the external shutter could not achieve a 1/500 second exposure time. For steps 1 and 3, the vacuum motor was removed from the camera body and was suspended from the ceiling of the aircraft vibration simulator, as indicated in Figure 7. In this manner, vital vacuum was retained through connecting rubber hoses while isolating the inherent vibrations of the motor. Where possible, the camera was operated in serial mode with automatic exposure interval control of about 5 seconds. A total of 60 exposures were made in the internal vibration phase of the test.

Sizeable oscillograph vibration recordings were taken under each test condition of the actual vibration frequency acceleration and velocity values detected by the transducers. The oscillograph was operated in blackout mode so that the traces could be developed and permatized on the Kodak Linagraph Direct Print Paper. While this mode allowed for permatized graphs of recorded vibrations, it prevented sample recordings of vibrations from being made for instant analysis. Sample recordings would have been desirable in preliminary testing of internal vibrations, and, later on, in the presetting of desired external vibration amplitudes.

III.B.3 External Vibration Phase

During the external vibration phase of the test, it was considered more important to know the characteristics of the vibrations received at the camera mount from external sources than to know what vibrations filter through the isolators and are received at the camera. For this reason, all transducers were relocated outside of the isolation system and were placed at the foot of the forward isolator (Figure 8) so as to record external vibrations being received.

Since the frequency spectrum under procedure XII of MIL-E-5272 indicates a frequency spectrum of 5 to 500 cps, it was decided to conduct the external vibration tests using frequencies of 5, 50 and 500 cps, which could be set directly on the vibration test equipment. The amplitudes, however, could not be set directly although they were continuously variable. Thus it was impossible to know at the time just what amplitudes of external vibrations were being applied. It was decided to use personal judgment at each frequency to select a low amplitude vibration to represent a routine vibration, plus a high amplitude vibration at what might be considered to be maximum rough conditions. This was done by sight, feel, and, in the case of the 500 cps vibrations, by sound. This rather unsophisticated approach, however, produced reasonable vibration amplitudes, as will be shown later.

Exposures were then made with externally applied and recorded vibrations at 5, 50 and 500 cps, at two amplitudes each, for low and high contrast targets, and with both 1/200 and 1/500 second exposures. This required 344 additional photographs.

IV. DATA PROCESSING AND ANALYSIS

IV.A Vibration Data

After the 400 feet of oscillograph paper was developed and permatized, it was found that one roll of recording paper had been developed improperly and the recorded information was destroyed. Fortunately, the roll contained recordings of internal vibrations. As the real purpose of the internal vibration phase was to study the effect, and not the size, of internal vibrations, the measurement of internal component vibration parameters was an unnecessary attempt to know more about the nature of those components. The internal motor operating frequencies were later obtained from the manufacturer as approximately 50 and 250 cps for the main and vacuum motors respectively.

A problem pertaining to the recording of external vibrations, however, was cause for concern. It was immediately noticed that recorded accelerations were very erratic, with many instances that the recorders went completely off-scale. The problem was analyzed by WPAFB Avionics Laboratory engineers to be one of improper grounding, which caused the accelerometers to pick up electrical signals from within the camera. The value of redundant instrumentation was proven, however, since the recorded data from the velocity transducers was completely sufficient for the determination of vibration amplitudes and accelerations from graph 1-9 of Harris and Crede [6].

The recordings used consisted of three sinusoidal waves for each test condition, one wave each for the x, y and z velocity pick-ups. The amplitudes of these waves were converted directly into vibration peak velocity values per calibration values established for the range of gain settings of the amplifier. The vibration frequency values were measured directly on the graph recordings as cycles/inch of graph paper multiplied by the inch/second chart speed of the recorder. Tables VI and VII are tabulations of recorded external vibration parameters for each test condition. In addition, Graphs 1 and 2 are plots of recorded vibrations as compared with the vibration spectrum graph from MIL-E-5272 Procedure XII as compiled by Casper [5]. Also shown is the vibration spectrum of a modern jet aircraft, the KC-135, military equivalent of the Boeing 707. Since the vibration spectrum includes those vibrations recorded during take-off and landings, the vibrations occurring during a photographic flight would be somewhat less severe. The test vibrations appear to fit quite well below the envelope of possible values; however, the high amplitude 5 cps vibrations are probably nearer to maximum conditions than would be tolerated on a photographic mission.

IV.B Resolving Power

IV.B.1 Resolution Determination

The film was uniformly developed in a Houston Fearless A-6 Continuous Processing Machine to a gamma of 1.6, which prior experience indicated would yield optimum sharpness. Resolution determinations in the x and y directions were made by two independent observers for each of the 404 photographs using a 120 power microscope. The target pattern numbers were converted to resolution values in lines/mm with calculations listed in Appendix A. Although the resolution determinations were purely a matter of personal judgment, nearly all determinations of the two sets agreed with each other within one test pattern.

The mean x and y resolution values of the 404 photographs are tabulated in Tables I through IV. Note that resolution values indicated in the left columns are the only resolution values possible from the various numbered resolving power patterns of the targets. The number of photographs indicated in a row between the tabulated resolution values is that number of times that one observer judged the higher value and one observer judged the lower value. Thus the between the line recording is in effect the mean of the two values. For example, in comparing the resolution values computed in Appendix A with those values listed in the first column of Table I, it can be seen that 67 lines/mm is obtained from resolution of target element 3 from group 2, while 60 lines/mm is obtained from resolution of target element 2 from group 2. Theoretically, no resolution value between 60 and 67 lines/mm can be observed. The number 1 written between the lines for 60 and 67 lines/mm (under the vacuum motor test condition of Table I) indicates that on one exposure, target 2-2 was read by one observer and target 3-2 by the other observer. While 63.5 lines/mm was not one of the discrete possible values, it would be reasonable to consider a resolution of 63.5 lines/mm as a mean of the two discrete values observed.

IV.B.2 Analysis of Results

In analyzing the results of the resolution determinations it is obvious that resolution in the upper ranges is extremely sensitive to the slightest disturbance. For example, the static photographs taken of the high contrast target indicate that resolutions up to about 160 lines/mm are possible, an indication of the fine grained film and the quality of the lens. Yet, under what was thought to be identical static conditions, resolutions as low as 128 lines/mm were recorded. With the low contrast target, resolution values of 48 to 57 lines/mm were recorded under "static" conditions. Obviously the camera was not truly static and was disturbed by vibrations from the vacuum motor transmitted through the flexible rubber hose, from other machinery running in the building or by human perturbations from a man standing on the simulator platform to advance the film when required.

The vacuum motor, which vibrates at about 250 cps, produced slight image degradation from the static test condition. The main motor, which vibrates at about 50 cps, produced greater image degradation generally, as can be seen in Tables 1 through 4. However, the combination of the two internal vibration motors rarely produced resolutions that were worse than from the individual components vibrating alone.

Since the internal vibrations were of fairly high frequency, the 500 cps external vibrations received at the mount did not degrade the image very often. In fact, the opposite result occurred in many cases. The system reacted as though it were better balanced as a result of this high frequency external excitation. Possibly, the external vibrations were of such frequency and magnitude that they served as a dynamic damping system which "broke up" the inertial rocking motion caused by the internal dynamic system of the camera. This theory is supported even stronger by the fact that high amplitude vibrations at 500 cps produced better resolution values generally than did the low amplitude vibrations at that frequency. This would indicate that the high amplitude 500 cps excitation did a better balancing job than did the lower amplitude vibration at that frequency. The author can furnish no explanation why this phenomenon was more pronounced with the high contrast target than with the low contrast target.

The 50 cps external excitations produced interesting resolution values. Again several of the high amplitude test conditions yielded better resolution values than the low amplitude test conditions; this time, however, the phenomenon was more pronounced with the low contrast target. Another interesting result is that the 50 cps test condition produced both expected image degradation in some photographs and unexpected image improvement in others. In several photographs the recorded resolution values equalled the highest value recorded under the static test condition; these exposures were evidently taken when the 50 cps external vibration was out of phase with, and effectively balanced, the 50 cps internal vibration from the main motor. In other words, the force vector from internal components was then approximately equal to but opposite in sign from the force vector from external excitation. Image degradation in the other photographs occurred in various degrees proportional to the vector addition of the various force vectors, reaching a maximum when the component forces are all maximum in the same direction.

The 5 cps external vibrations proved what had been expected all along - that low frequency vibrations are the most damaging. Resolution values of the low contrast targets degraded in the range from 60 to 10 lines/mm for the same test condition, and resolution of the high contrast target degraded in the range from 143 to 8 lines/mm.

By the same test condition, it is meant that with the same target, the same camera settings and the same steady state external excitation from the aircraft vibration simulator, the camera is set in serial mode operation and all 3,5 or 20 exposures are made without changing any of the parameters. The large disparity of resolution values for each test condition is then a result of the phase angle combinations or vector additions of the various forces occurring in the camera at the instant of exposure, as explained in section II and Appendix C.

In all cases, the faster exposure time proved to be more effective in combating image motion. This result was fully expected since resolution degradation is a direct function of vibrational image velocity multiplied by exposure time.

IV.B.3 Resolution Prediction

The theoretical prediction of resolution values could be performed by any organization experiencing or anticipating a possible resolution degradation problem resulting from vibrations or unknown causes. Little additional information is required beyond what is normally available to an organization with an aerial camera. The theory and requirements are listed in Appendix D for those with further interest in this subject. Several interesting conclusions can be drawn from the analyses of Appendix D, and these are listed with Section V of this report.

IV.C. Acutance

IV.C.1 Calibration of Microdensitometer

As was mentioned previously in section III.B.1, each strip of film was exposed to a density step wedge. This wedge was a glass plate containing twenty-one sections with uniform densities varying from clear to completely opaque. Although each strip of film was developed in a Houston

Fearless Continuous Processing Machine to a gamma of 1.6, it is possible that slight differences in development could affect the acutance determinations. Thus, it was necessary to calibrate the microdensitometer separately for each strip of film. Each step of the step wedges on each film strip was measured twice on a Macbeth TD-102 Quanta Log Densitometer, which had previously been calibrated to NBS standards. This is a densitometer which measures diffuse transmission density integrated over a rather large portion of each step of the wedge. It was found, however, that repeatability was excellent, as measurements made at either end of the steps were virtually the same.

Actual scanning of edges was to be performed with the Mann-Data Micro-Analyzer. This microdensitometer is shown in Figure 9 on the right, with chart recorder in the center and magnetic tape recording unit on the left.

Before calibration of the microdensitometer could begin, it was necessary to decide on the size and shape of the scanning aperture. Magnified views of the edge scan pattern (the large nearly square black pattern of the target shown in Appendix A) of the poorest resolved photographs indicated that the vibrations did in fact cause the edges to have narrow streaks or steps of differing densities parallel and immediately adjacent to the pattern edges. In order to scan and measure these streaks, it was mandatory that the edge be scanned with a slit as opposed to a circular shaped aperture which would integrate the density over the area of the circle. The circular shape would only suffice if the micro-dot mode were used, but a much larger aperture area was required to eliminate most of the granularity "noise." Several dozen slit width and length possibilities were tested in an attempt to remove most of the granularity "noise" while using the narrowest slit possible for best edge measurement. It was decided that the optimum slit was one with a width of 3 micro-meters and a length of 502 micro-meters. This length was approximately one half of the side dimension of the edge scan pattern.

As each strip of film was introduced to the microdensitometer, calibration was performed by scanning back and forth along the steps of the wedge, adjusting the gain settings until the average recorded density for each step best fit the density values for those steps as recorded with the Macbeth densitometer.

IV.C.2 Scanning

Because of economic considerations, it was decided to scan only those edges of photographs which indicated maximum or minimum resolution values for each test condition. This required a total of 144 edge scans of a possible 808.

After the microdensitometer was calibrated, the appropriate photographs were advanced to be scanned. All horizontal scans were made of the left edge of the edge scan pattern: all vertical scans were made of the bottom edge of the edge scan pattern. The biggest problem involved was the alignment of the scanning slit parallel with the edge to be scanned. This problem alone took more than half of the total scanning time. In addition to the angular alignment, it was necessary to align the slit so that the center of the edge was scanned. After this angular and linear alignment was accomplished, the slit was "backed off" from the apparent edge by 60 micro-meters. Scanning was then accomplished by taking 40 density readings at the 3 micro-meter intervals over the 120 micro-meter scanning distance of each of the 144 edges to be scanned. (A scanning distance of 120 micro-meters was used because it was found that the edge scan pattern of the poorest resolved target appeared to have a lateral edge blur of nearly 100 micro-meters, as measured on the microdensitometer, and the expected sigmoid shape of the trace needed overages at either end in order to flatten out.) Using a 3 micro-meter wide slit, the 3 micro-meter sampling interval enabled complete scanning of the edge for optimum integration of density values without sample area voids and overlaps as would be encountered with a circular aperture.

A diagram of the procedure used in scanning a vertical edge is shown in Figure 10. In order to scan the horizontal edge, the photograph would be rotated approximately 100 grads, the slit and edge would be realigned, and the same basic procedure would be repeated.

IV.C.3 Acutance Determination

Although the scans generally produced the expected sigmoidal shape, including edge effects, many of the edge traces had "steps" part way up the sigmoid where the gradient was temporarily small and even negative. These steps had been seen on the negatives under high magnification, were evident on the recording chart paper and were verified by the magnetic tape "dump" of density recordings. The acutance of each edge trace was computed as follows.

IV.C.3.a Acutance Formula Method

The acutance of each edge trace was computed using the modified acutance formula of Jones and Higgins [7]. This procedure is explained in Appendix E. The formula indicated in Figure E.1 would appear to provide an objective indication of image sharpness; however, the gradient steps along the sigmoid created problems in that it was often difficult to distinguish gradient steps near the .005 gradient limit for points A and B along the curve, from the granularity noise which also starts near these points and has the same effect. It then became necessary to make a human decision in deciding where the points A and B occurred. This human decision removed complete objectivity from the process, and differing decisions were found to produce 30 to 40 % disparity of acutance values.

IV.C.3.b <u>Curve Fitting Method</u>

In order to obtain completely objective acutance values, an attempt was made to fit the density VS. scanning distance values to an arctangent and to a hyperbolic tangent curve by the method of least squares. These were the most common curves that had the general sigmoid shape.

This procedure, also explained in Appendix E, had the aim of determining the parameters of the smooth curve which best fit the recorded values; one could then measure the acutance from the parameters of this best fitting smooth curve. This would eliminate all complications caused by the granularity noise and gradient steps, and would produce a unique acutance value for each scan, obtained through complete objectivity.

This method produced results which generally agree (within 25% approximately) with results using the acutance formula method and unaltered data; however, some values disagreed by as much as 100% and even more. While unique acutance values were obtained, the variance of unit weight indicated a very poor fit of some data to the design curve, particularly those with more pronounced edge effects. In effect, the same scans that produced questionable results with the acutance formula method also produced a poor fit to the arctangent and hyperbolic tangent curves, and produced large discrepancies with the acutance formula method values. Indeed, the fallacy of the curve fitting method is that there is in fact no reason why the data should fit the mathematical model used, particularly since the edge effect is a very real characteristic of an edge trace which should not be artificially removed.

The curve fitting method was abandoned and the acutance formula method used with guidelines established for selection of points A and B nearest to the leveled-off density values beyond the edge effects.

IV.C.4 Analysis of Results

If the computational method of acutance determination was bewildering, the results were even more so. Although there was a modest trend throughout the data of acutance degradation being directly proportional to resolution degradation, this trend was definitely expressed only for those photographs with resolution values poorer than 50 lines/mm. For photographs with resolution values in excess of 70 lines/mm, the results appear virtually random, i.e., approximately one-half of the maxima-minima condition pairs indicated better acutance for the poorer resolved target, and vice versa. Even after meaning the acutance values of all photographs with the same resolution values, as was done at Table V, the acutance values can be seen to have unsystematic correlation to the related resolution values over much of the table. While the meaning process would smoothen out any small irregularities in the data, it is obvious that there are either large data acquisition irregularities, or else a point is reached where the two quality parameters are in fact uncorrelated. This latter possibility will be investigated first.

Higgins and Wolfe [8] photographed a similar type of test target in various parts of the field of the lens at a series of focal settings. They found some images where resolution was high and sharpness was low, and others where resolution was low and sharpness high. While vibrations should in no way change the metrically stable interior orientation of the camera, a similar type of phenomenon could possibly occur. If the focusing of the camera can so affect the spread function (reference James and Mees [1], page 501) that its shape or degree of light mounding at one setting is optimum for resolving power, and its shape at another focal setting is optimum for sharpness, it would appear possible that vibrations could randomly shake a spread function either toward or away from its optimum shape for sharpness, which is known to differ from its optimum shape for resolving power. Furthermore, it is possible that a random adjustment in the shape of the spread function, in the direction of improved acutance, could be so strong that it reaches and exceeds the optimum shape for image sharpness, producing degradation in an opposite sense. This would account for the correlation between low resolution and low acutance values, both being produced by unusually strong adjustment of the spread function.

A more logical explanation, however, might be that gross errors did occur in the data acquisition phase of the acutance determinations. More specifically, it is possible that the investigator failed to obtain the optimum parallel alignment of the scanning slit and edge that he attempted to achieve. It was known from the microdensitometer instruction manual that a 1 x 300 micro-meter slit, measuring a 100 line/mm edge, gives a 50% error in acutance from a mere 30 arc-second misalignment angle. Although more than half of the total scanning time was spent in attempted alignment, it is possible that either a better alignment procedure should have been used, or else the scanning slit itself was not aligned with the index mark used for this purpose.

One method of overcoming this problem might be to track the scan three times with rotation of a few seconds in either direction in addition to the center orientation. Only if the center orientation produces the greatest acutance of the three scans, and the rotation angles approach zero, can one be assured that optimum alignment has been achieved. This, however, could require a great many scans for each edge which would be impractical for analyses of numerous edges. It might be better to scan with a circular shaped aperture and accept the fact that the resulting scan is a poor representation of the vibrated edges.

V. CONCLUSIONS

In order to best express the conclusions of this study, it is necessary to provide a generalized listing of resolution degradations resulting from the vibration test conditions, summarized from Tables I through IV. As this study is concerned with the poorest results that might be expected from any test condition, the degradations listed will pertain to the poorest recorded resolution values in either the x- or y-directions, for each test condition.

With the low contrast target, the static resolving power capability was found to be 67 lines/mm. The maximum degradation for the total internal as well as external excitations were found to be as follows:

Test Condition	Exposure Time 1/200 Sec.	Exposure Time 1/500 Sec.
Total Internal Vibrations	36 %	32 %
External Vibrations:		
500 cps, low amplitude	28 %	28 %
500 cps, high amplitude	28 %	24 %
50 cps, low amplitude	40 %	32 %
50 cps, high amplitude	32 %	28 %
5 cps, low amplitude	43 %	36 %
5 cps, high amplitude	84 %	64 %

With the high contrast target, the static resolving power capability was found to be 160 lines/mm. The maximum degradation for the total internal as well as external excitations were found to be as follows:

Test Condition	Exposure Time 1/200 Sec.	1/500 Sec.
Total Internal Vibrations	41 %	41 %
External Vibrations:		
500 cps, low amplitude	47 %	41 %
500 cps, high amplitude	37 %	33 %
50 cps, low amplitude	47 %	41 %
50 cps, high amplitude	56 %	47 %
5 cps, low amplitude	66 %	44 %
5 cps, high amplitude	95 %	88 %

The conclusions of this study are the following:

1. High contrast images are more easily degraded by vibrations than are low contrast images.

2. Internal vibrations of a camera system do cause rather large degradations of image quality. Furthermore, the internal vibration parameters will add to or subtract from external vibration parameters at random, the net result being dependent upon the phase angles of the various contributing (sinusoidal type) forces at the time of exposure.

3. A single vibrating condition will produce serial photographs possessing a great disparity in image quality. For example, while undergoing the same vibrations, one exposure could resolve 160 lines/mm, while the very next exposure could resolve 8 lines/mm. This disparity of results is particularly critical when the exposure time is quicker than the period of the vibrations acting on the camera system.

4. Image quality degradation in the direction of flight on the photographs is somewhat independent from image quality degradation in the cross-flight direction. While both degradations are dependent upon the same vertical vibration accelerations, the same (Dz) vertical moment arm of unbalance and certain isolator characteristics, many contributing parameters are independent for the two directions. Some of the independ-

ent parameters are the following:

a. Independent vibration accelerations in the longitudinal and lateral directions (see Tables VI and VII).

b. Different longitudinal (Dx) and lateral (Dy) moment arms of unbalance between the center of gravity of the camera and the elastic center of the isolation system (see section II).

c. Different longitudinal and lateral camera dimensions and isolator spacings, as well as different isolator loadings. These factors contribute to different isolation system natural frequencies which significantly affect the different angular rotations which cause image quality degradation.

5. Some medium and high frequency external excitations can actually improve image quality. This could be done by "breaking up" internal vibration resonance or by balancing internal vibrations with out-of-phase vibrations of the same general frequency. It is also possible that the mass inertia of the camera, mounted on a low natural frequency isolation system, is such that the camera is physically incapable of following the path of the external vibrations at higher frequencies and amplitudes. (This would be similar to an automobile, with a low natural frequency suspension system, remaining fairly steady while its tires are bouncing violently on a rough road.) The net effect is that an element of balance is achieved and resolution is improved.

6. Medium to low frequency vibrations can be extremely damaging to image quality. Resolution loss, as high as 95%, could be experienced from vibrations at the extreme range of expectancy for a photographic mission, with a related acutance loss of 93%.

7. Although increased exposure speed consistently improves image quality in a dynamic situation, the improvement in results is not as great as would be expected. The 2 1/2 time faster exposure times provided an average relative improvement in resolution degradation of 13.5%, with maximum relative improvement of 30%.

8. Image sharpness, or acutance, varies directly with the resolution as degraded by vibrations. The proportionality becomes more pronounced as image degradation increases as a result of stronger vibrations. This conclusion is drawn, however, with the knowledge that the data contained limitations imposed by the practical inability to obtain optimum orientation of the scanning slit when scanning the edges.

9. Camera systems could definitely be designed so as to minimize the influence of vibrations; recommended improvements are listed in Section VI.

VI. RECOMMENDATIONS

In an attempt to lessen the image quality degrading influence of vibrations on aerial camera systems, the following recommendations are made.

VI.1 Existing Camera Systems

It is assumed that any operator would use the largest aperture and fastest exposure time settings available for the film, lighting conditions etc. The common sense rule for improved image quality with existing camera systems is to avoid turbulent weather conditions and to avoid taking photographs if the camera operator can see the camera rocking or can feel strong vibrations under-foot. If these conditions cannot be avoided, any mechanical engineer could determine where to attach weights to the camera so as to move the center of gravity of the camera as close as possible to the elastic center of the isolation system.

In all cases, the most expedient method of controlling image degradation would be to have the camera operator hold the camera as steady as possible with his hands. The human body remains the best shock absorber known to man.

VI.2 Future Camera Systems

The following principles should be followed in the design of future aerial camera systems.

1. The camera body should be attached to the mount in such a way that the center of gravity of the camera with loaded magazine falls in

the same horizontal plane as the center of the vibration isolators.

2. Heavier internal components should be located so as to bring the center of gravity of the system as close as possible, as permitted by other design requirements, to the elastic center of the vibration isolators.

3. If the isolators receive different loading, the spring constants and damping factors should be carefully matched to each other.

4. Isolation systems with low natural frequencies should be used.

5. Faster exposure time capabilities should be developed, providing shutter efficiency is retained.

VI.3 Future Study

It is recommended that studies of this general nature be performed and expanded to analyze the effects of vibrations on the Modulation Transfer Function as well as the effects on image quality parameters at off-axis positions of the format.

VII. FIGURES, GRAPHS, and TABLES

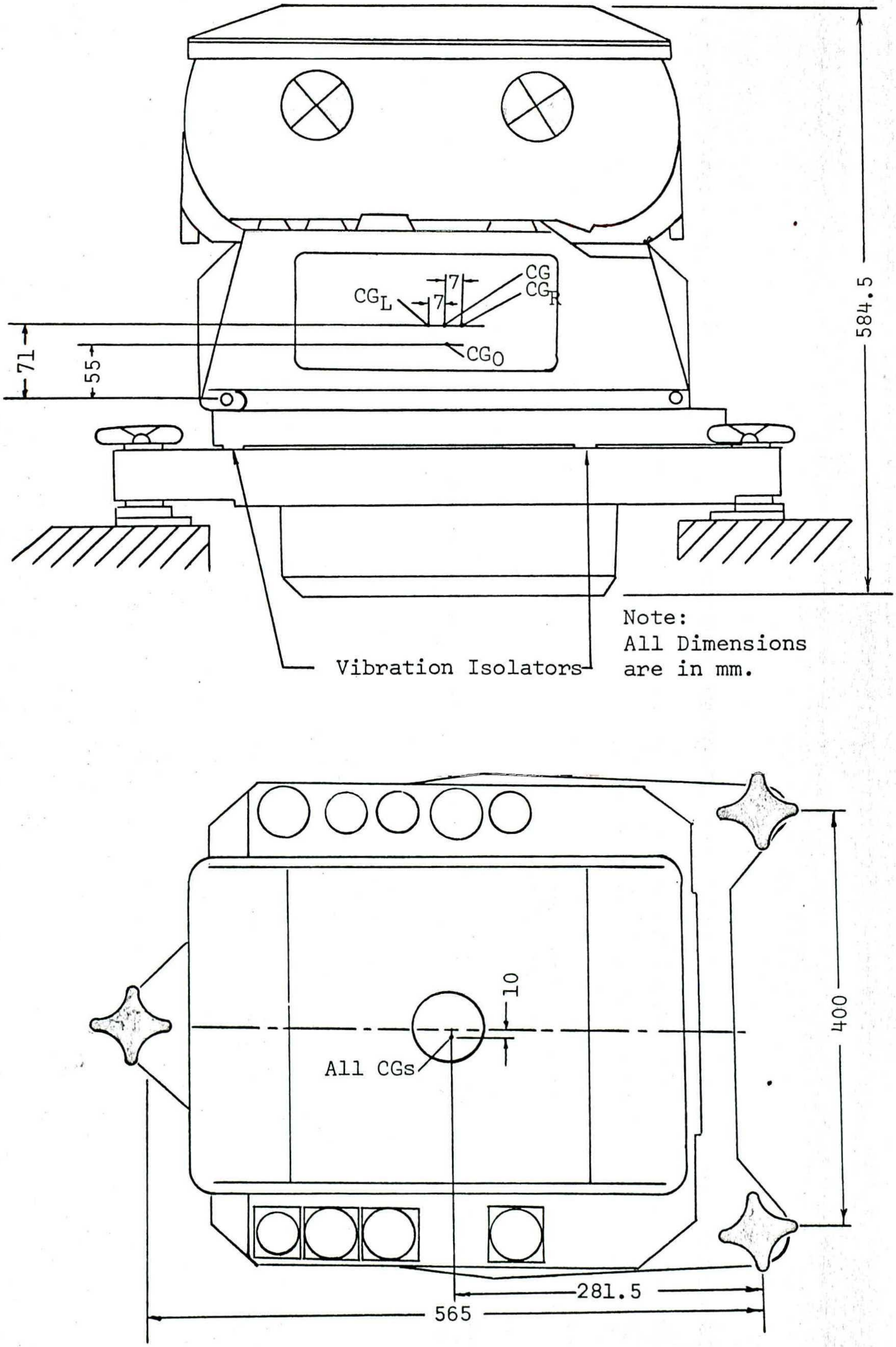

Figure 1 - Diagram of Zeiss RMK AR 15/23 Camera

Figure 2 - Characteristic Curves of Vibrachoc Isolators

Figure 2.1
Load - Deflection Curve

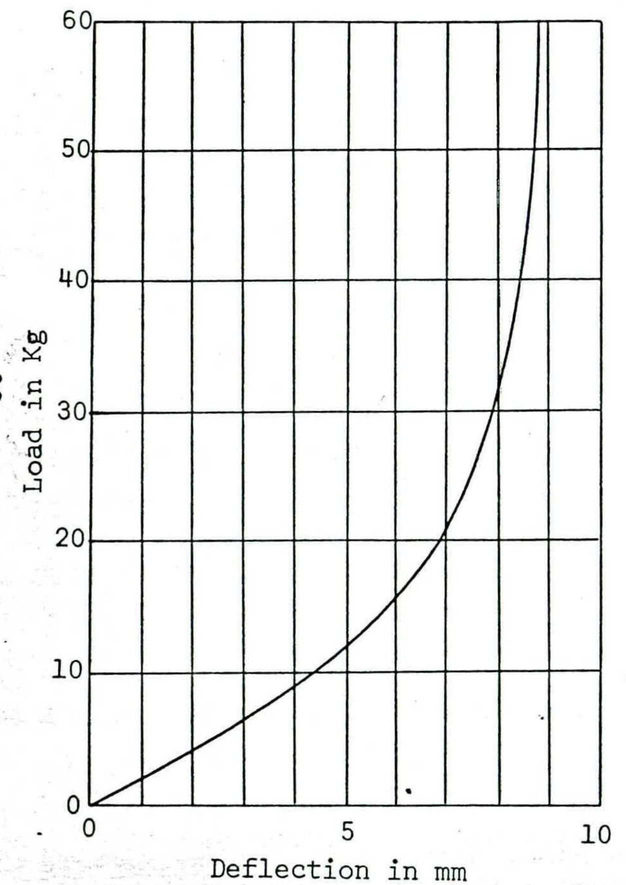

Figure 2.2
Characteristic Curve for a System with 1 Degree of Freedom

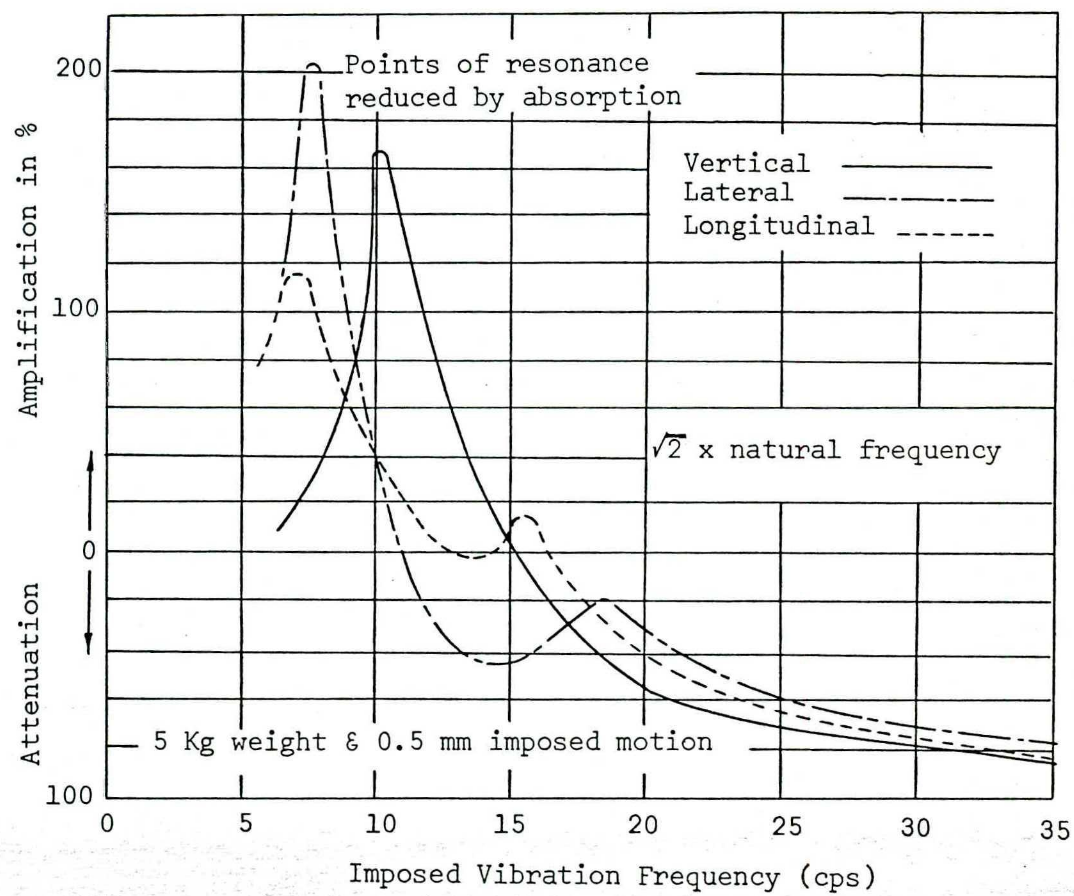

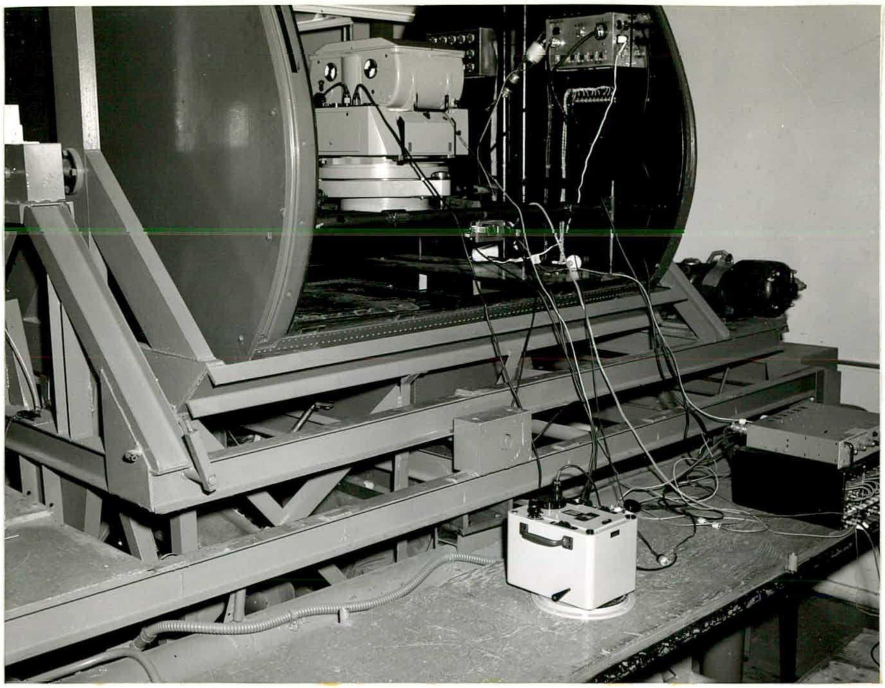

Figure 3 - Aircraft Vibration Simulator

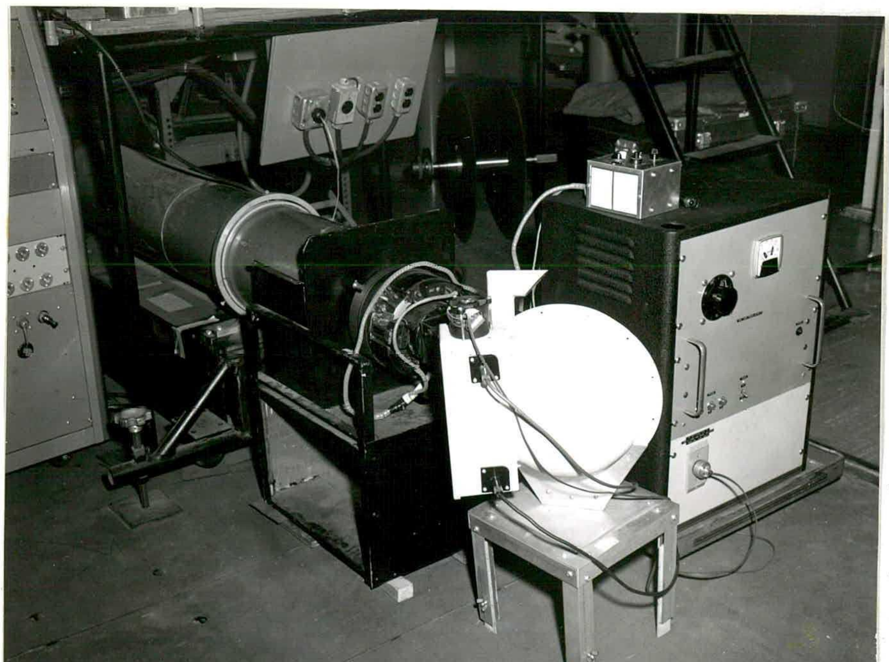

Figure 4 - Light Source, External Shutter and Collimator

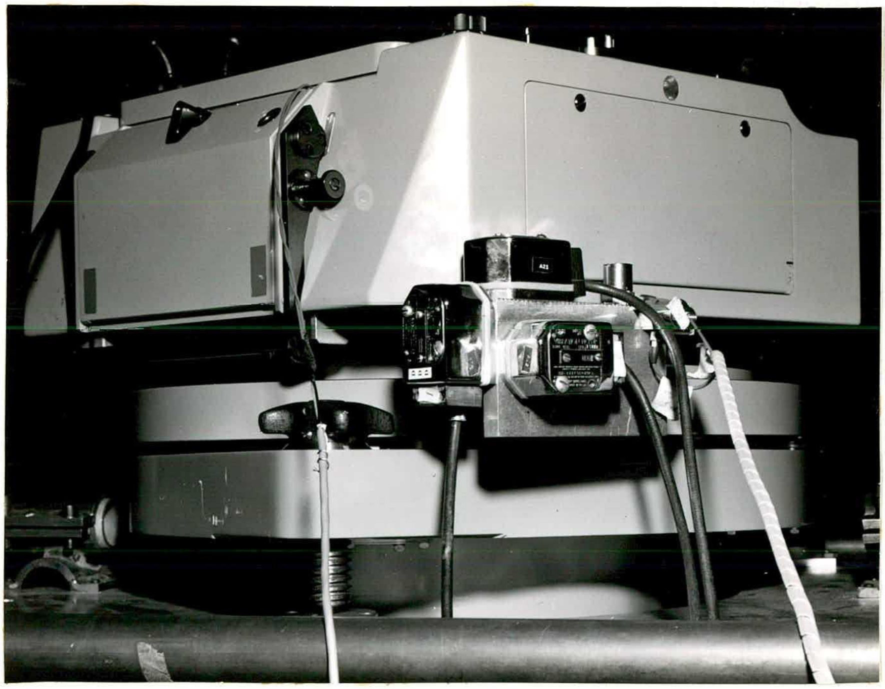

Figure 5 - Transducer Assembly for Internal Vibration Recording

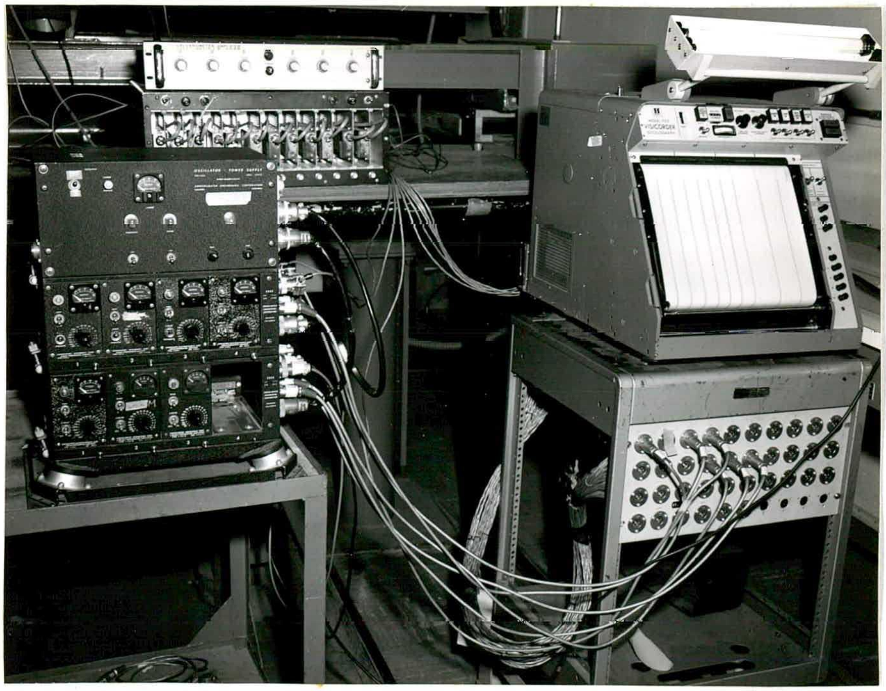

Figure 6 - Vibration Recording Equipment

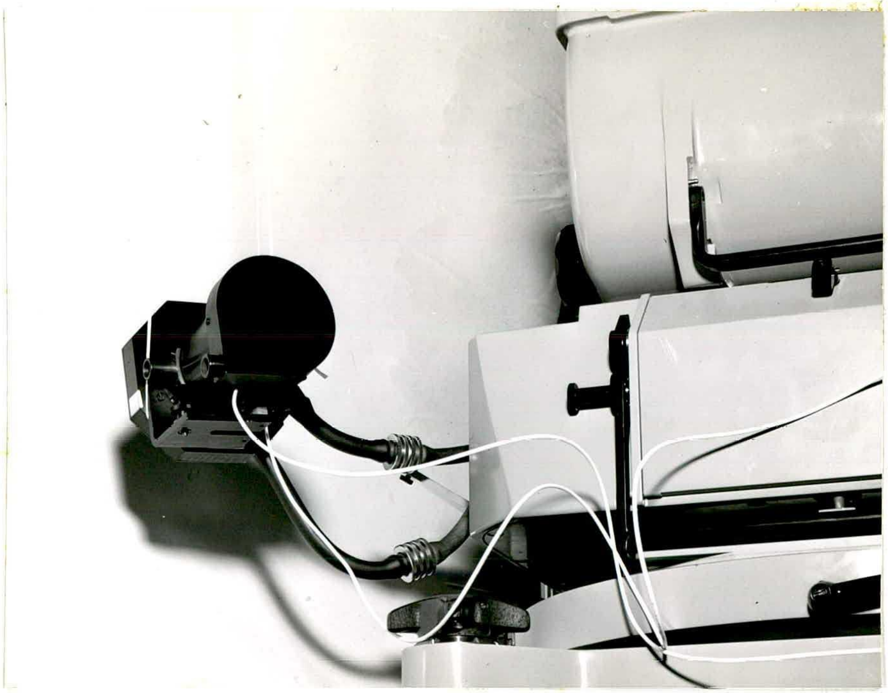

Figure 7 - External Operation of Vacuum Motor

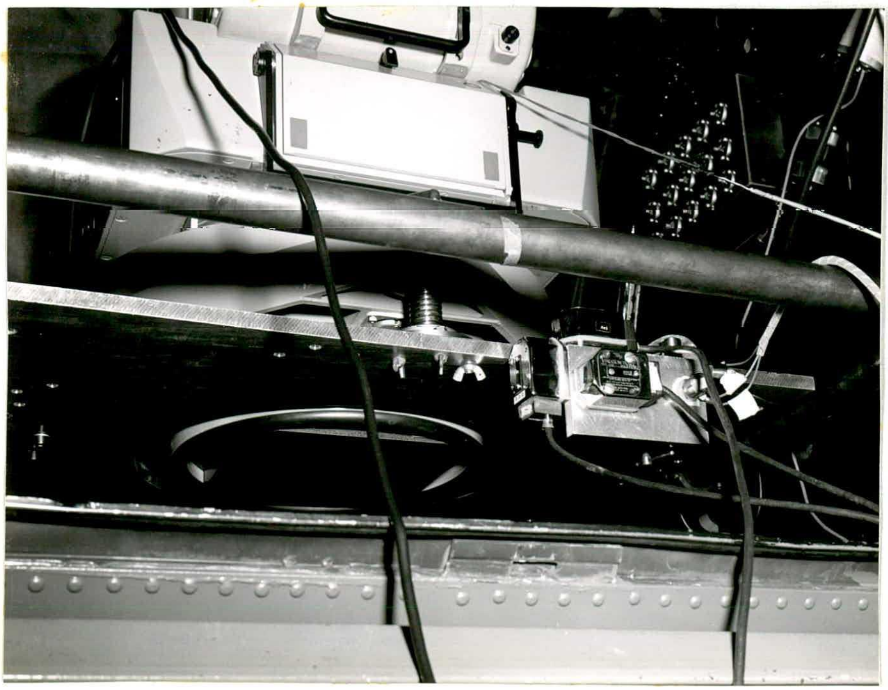

Figure 8 - Transducer Assembly for External Vibration Recording

Figure 9. Mann-Data Micro-Analyzer with Auxiliary Equipment

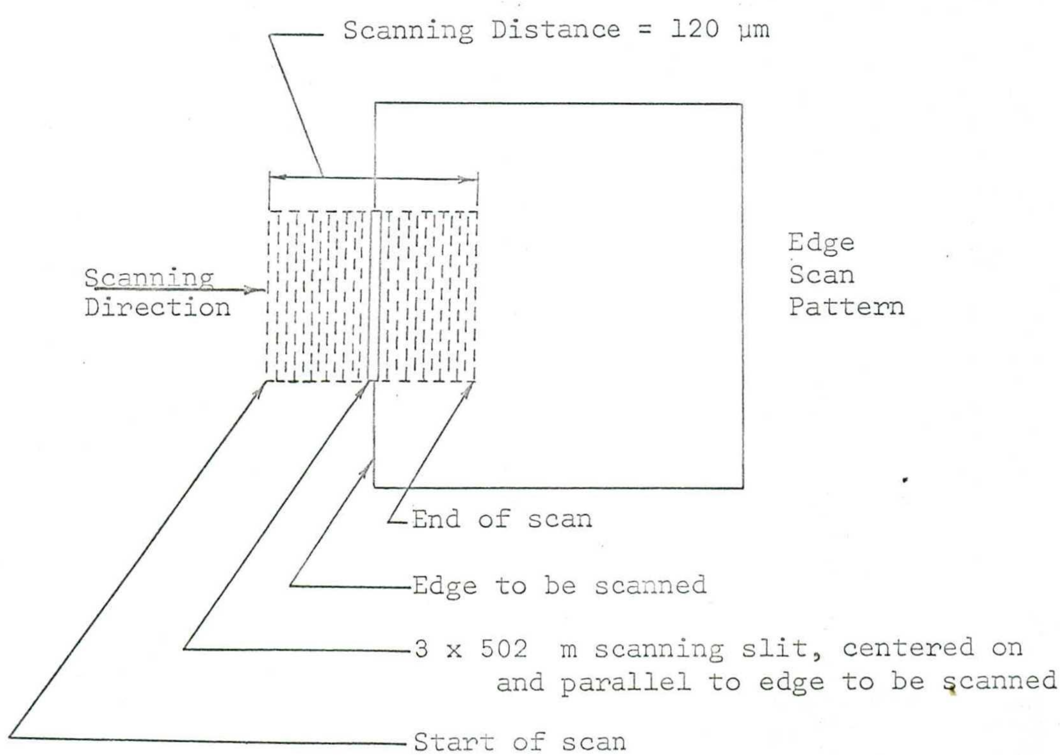

Figure 10. Diagram of Scanning Procedure

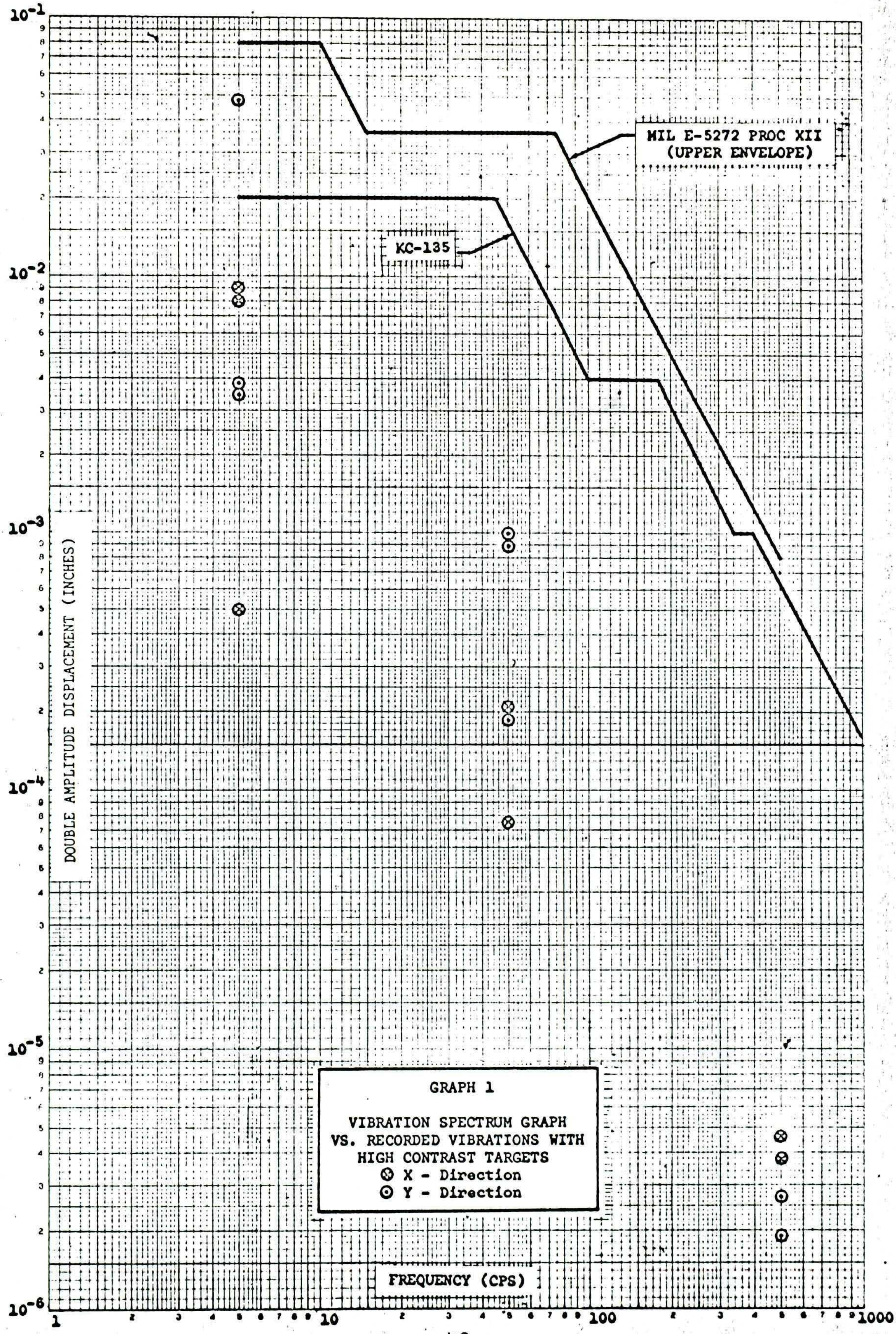

GRAPH 1

VIBRATION SPECTRUM GRAPH VS. RECORDED VIBRATIONS WITH HIGH CONTRAST TARGETS
⊗ X - Direction
⊙ Y - Direction

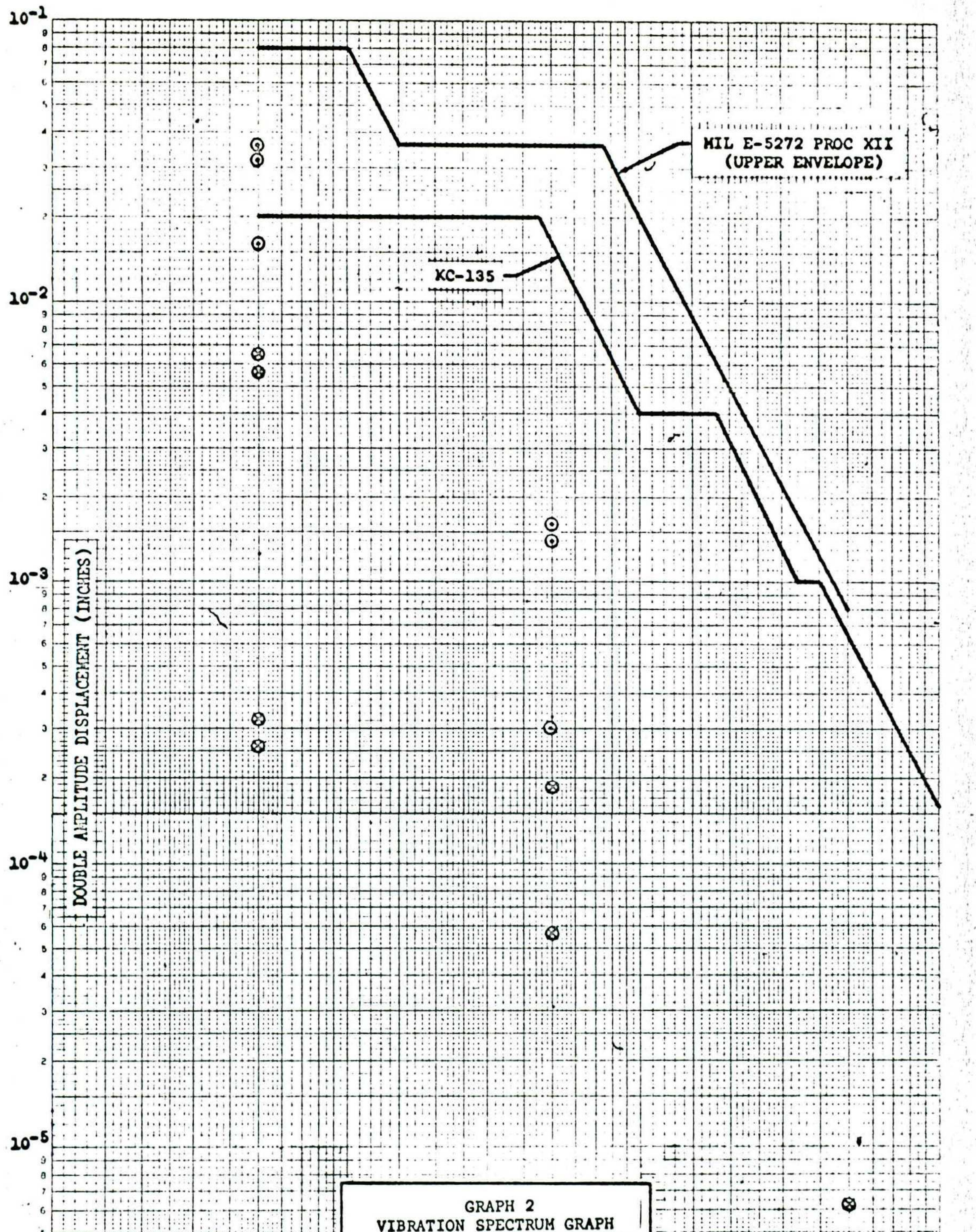
MIL E-5272 PROC XII
(UPPER ENVELOPE)
KC-135
DOUBLE AMPLITUDE DISPLACEMENT (INCHES)
FREQUENCY (CPS)
10^-1
10^-2
10^-3
10^-4
10^-5
10^-6
1
10
100
1000
GRAPH 2
VIBRATION SPECTRUM GRAPH
VS. RECORDED VIBRATIONS WITH
LOW CONTRAST TARGETS
⊗ X - Direction
⊙ Y - Direction

TABLE I - LOW CONTRAST TARGET

NUMBER OF PHOTOS WITH X-DIRECTION RESOLUTIONS INDICATED

	1/200 Sec. exposure time										1/500 Sec. exposure time							
Resolution Lines/mm	Static	Vacuum Motor	Main Motor	Total Internal	500 cps lo ampl	500 cps hi ampl	50 cps lo ampl	50 cps hi ampl	5 cps lo ampl	5 cps hi ampl	Main Motor	Total Internal	500 cps lo ampl	500 cps hi ampl	50 cps lo ampl	50 cps hi ampl	5 cps lo ampl	5 cps hi ampl
67	1							1										
		1												1				
60													2	1		3	1	
	2			1			1				1			1		1		
54	1		1	1	1	2	.2	9	2			1			6	3	5	1
	1	1	2				5	3•	4						3	3	2	
48		2	2	1	2	1	7	6	11	2	4	3	1		9	10	10	5
				1			3	1	2			1			2			4
43		1		1			1		1								2	6
							1			2								3
38										3								1
34										4								
										3								
30										5								
										1								
27																		
Totals	5	5	5	5	3	3	20	20	20	20	5	5	3	3	20	20	20	20

Note: Resolution values indicated are the only values possible from the targets themselves. Any number written on a line between resolution values indicates the number of times that one observer recorded the higher value while the other observer recorded the lower value.

TABLE II - LOW CONTRAST TARGET
NUMBER OF PHOTOS WITH Y-DIRECTION RESOLUTIONS INDICATED

	1/200 Sec. exposure time										1/500 Sec. exposure time							
Resolution Lines/mm	Static	Vacuum Motor	Main Motor	Total Internal	500 cps lo ampl	500 cps hi ampl	50 cps lo ampl	50 cps hi ampl	5 cps lo ampl	5 cps hi ampl	Main Motor	Total Internal	500 cps lo ampl	500 cps hi ampl	50 cps lo ampl	50 cps hi ampl	5 cps lo ampl	5 cps hi ampl
67							1					1				1		
60							1	2 5					1	1		4 2	3	
54	1 2	1			1	1	4	2 3	5		2		1 1	1	3 8	1 8	4 5	1 3
48	2	3	2 2	2 3	1 1	2	5 6	3 5	1 7	1	2 1	3		1	3 5	2 2	2 4	2 2
43		1					2		5 1	2 1		1			1		1 1	1 1
38			1				1		1	1 1								4 1
34																		1
30										1								1
27										1 1								2
24																		1
21										1 2								
19										3								
17										1								
15										1								
13										2								
12																		
11																		
10										1								
Totals	5	5	5	5	3	3	20	20	20	20	5	5	3	3	20	20	20	20

TABLE III - HIGH CONTRAST TARGET
NUMBER OF PHOTOS WITH X-DIRECTION RESOLUTIONS INDICATED

	1/200 Sec. exposure time										1/500 Sec. exposure time							
Resolution Lines/mm	Static	Vacuum Motor	Main Motor	Total Internal	500 cps lo ampl	500 cps hi ampl	50 cps lo ampl	50 cps hi ampl	5 cps lo ampl	5 cps hi ampl	Main Motor	Total Internal	500 cps lo ampl	500 cps hi ampl	50 cps lo ampl	50 cps hi ampl	5 cps lo ampl	5 cps hi ampl
169																		
	1																	
151																		
	1	1																
135	2						1		1			1						
	1					1								1				
120		1	1			1	1		1		1	2		1			1	
				1		1			2		1		1				1	1
107		3	1				6	4	5		2	2	1	1	8	2	1	4
			2	1			2	2	2						3	4	3	1
95			1	3	1		7	6	9	1	1		1		9	6	13	4
								5		1						5	1	1
84					2		3	3		2						3		3
																		1
75										1								
67																		2
										1								
60										1								2
54										2								1
										2								
48										1								
43																		
38																		
34																		
										2								
30										4								
										1								
27										1								
Total	5	5	5	5	3	3	20	20	20	20	5	5	3	3	20	20	20	20

TABLE IV - HIGH CONTRAST TARGET
NUMBER OF PHOTOS WITH Y-DIRECTION RESOLUTIONS INDICATED

	1/200 Sec. exposure time										1/500 Sec. exposure time							
Resolution Lines/mm	Static	Vacuum Motor	Main Motor	Total Internal	500 cps lo ampl	500 cps hi ampl	50 cps lo ampl	50 cps hi ampl	5 cps lo ampl	5 cps hi ampl	Main Motor	Total Internal	500 cps lo ampl	500 cps hi ampl	50 cps lo ampl	50 cps hi ampl	5 cps lo ampl	5 cps hi ampl
169																		
151	2	1																
																		1
135	1																	
	2					1					1			2				
120		3							5		1	1					1	1
			1				1				1		1		1		1	
107		1	3	1		1	3	1	3		2	2	1	1	4	2	5	
				3		1	7	1	1	1		1			5	7	4	3
95			1	1	1		6	9	6			1	1		10	10	9	4
					2		2	2										
84							1	4	1	1						1		
								2										
75									1	1								1
								1										
67									1									1
										2								
60										1								
54									2									
48										3								
43										2								
38																		
34																		2
										1								
30																		1
27										1								1
										1								
24																		
21																		2
19																		3
17																		
15																		
13																		
										1								
12																		
11										1								
10																		
9										2								
8										2								
Total	5	5	5	5	3	3	20	20	20	20	5	5	3	3	20	20	20	20

TABLE V

Resolution in lines/mm	Mean Acutance x 10^4	Sample size
160	28.71	1
151	22.60	2
143	25.39	2
135	24.66	3
127	21.59	6
120	27.00	6
113	23.86	6
107	23.30	12
101	24.51	2
95	23.16	15
90	31.80	2
85	24.58	6
71	22.17	1
67	11.94	3
63	5.17	1
60	10.88	8
57	12.27	8
53	12.70	14
50	12.08	6
48	13.06	17
45	12.86	4
42	12.68	5
40	9.90	3
38	11.82	2
28	8.86	2
24	8.62	1
19	4.95	1
10	4.49	1
8	2.23	1

TABLE VI
EXTERNAL VIBRATION DATA
FOR EXPOSURES OF LOW CONTRAST TARGET

Exposure Time	Frequency (cps)		500		50		5	
	Amplitude Category		Low	High	Low	High	Low	High
1/200 Sec. Exposure Time	Recorded Velocity (in./sec.)	X	.0060	.0070	.030	.030	.004	.108
		Y	.0026	.0040	.047	.260	.025	.498
		Z	.0040	.0050	.078	.146	.042	.228
	Double Amplitude (inches)	X	.0000038	.0000044	.000186	.000186	.00026	.0066
		Y	.0000016	.0000026	.00300	.00160	.00160	.0320
		Z	.0000026	.0000032	.000480	.00090	.00270	.0146
	Acceleration/Gravity (g's)	X	.049	.057	.025	.025	.00031	.0085
		Y	.021	.033	.038	.210	.00200	.0400
		Z	.033	.042	.064	.125	.00340	.0190
1/500 Sec. Exposure Time	Recorded Velocity (in./sec.)	X	.0060	.0100	.0090	.030	.005	.090
		Y	.0026	.0040	.0498	.220	.020	.564
		Z	.0040	.0070	.0480	.160	.033	.228
	Double Amplitude (inches)	X	.0000038	.0000062	.000056	.000186	.00032	.0056
		Y	.0000016	.0000026	.000320	.00140	.00124	.0360
		Z	.0000026	.0000044	.000310	.00100	.00220	.0146
	Acceleration/Gravity (g's)	X	.049	.080	.0073	.025	.0004	.0071
		Y	.021	.033	.0400	.180	.0016	.0450
		Z	.033	.057	.0390	.130	.0026	.0190

TABLE VII
EXTERNAL VIBRATION DATA
FOR EXPOSURES OF HIGH CONTRAST TARGET

Frequency (cps)			500		50		5	
Amplitude Category			Low	High	Low	High	Low	High
1/200 Sec. Exposure Time	Recorded Velocity (in./sec.)	X	.0060	.0070	.012	.030	.008	.144
		Y	.0030	.0040	.036	.160	.060	.780
		Z	.0048	.0050	.036	.130	.050	1.320
	Double Amplitude (inches)	X	.0000038	.0000047	.000076	.000186	.0005	.0092
		Y	.0000019	.0000026	.00022	.0010	.0038	.0480
		Z	.0000030	.0000032	.00022	.00082	.0032	.0840
	Acceleration / Gravity (g's)	X	.048	.057	.010	.025	.00065	.012
		Y	.025	.033	.030	.130	.0048	.062
		Z	.039	.040	.030	.110	.0040	.110
1/500 Sec. Exposure Time	Recorded Velocity (in./sec.)	X	.006	.007	.012	.030	.008	.120
		Y	.003	.004	.030	.140	.055	.780
		Z	.008	.006	.039	.120	.045	1.140
	Double Amplitude (inches)	X	.0000038	.0000047	.000076	.000186	.0005	.008
		Y	.0000019	.0000026	.000186	.00088	.0035	.048
		Z	.0000050	.0000038	.000240	.00075	.0029	.072
	Acceleration / Gravity (g's)	X	.048	.057	.010	.025	.00065	.010
		Y	.025	.033	.025	.118	.0045	.062
		Z	.065	.048	.031	.098	.0035	.092

APPENDIXES

APPENDIX A

USAF Resolving Power Test Target With Calculations

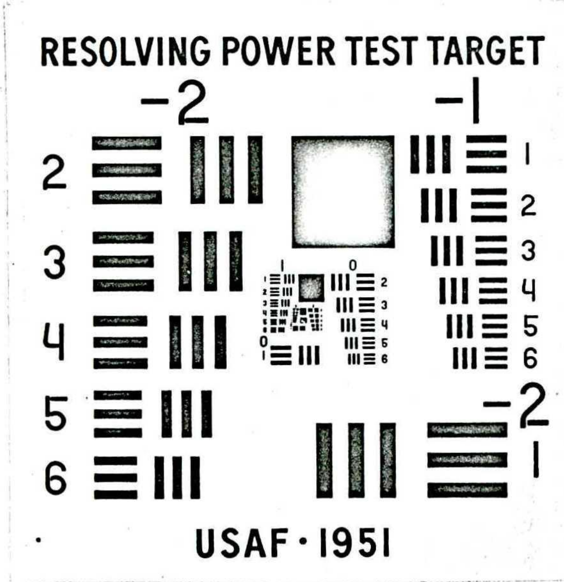

The USAF Resolving Power Test Target, as shown, consists of 10 target groups, every two target groups forming a square. There are 5 squares of different size, the smaller squares being inside the next larger ones. Every target group consists of 6 target elements.

The groups are designated by group numbers k. For example, -1, 0, +1, +2 and +3 in the range observed for this study. The elements are designated by element numbers n; n is equal to 1, 2, 3, 4, 5 or 6. The dimensions of the elements are such that the element number n within group number k represents a resolving power of

$$R = 2^{\left(k + \frac{n-1}{6}\right)} \text{ lines/mm.}$$

The resolving power of elements having the same element number, but belonging to groups of subsequent group numbers differ by the factor 2. Within a group, the resolving powers in subsequent elements differ by a factor 1.122, equal to the sixth root of two.

Because the scale of the target is reduced at photo scale by the ratio of camera constant divided by collimator constant, any target pattern read at photo scale would actually represent a resolving power of R x 80"/6".

The following target element numbers, within the range observed for this study, represent the resolution values in lines/mm observed at photo scale.

	Group Number (k)				
Element No. (n)	-1	0	+1	+2	+3
1	7	13	27	54	107
2	8	15	30	60	120
3	9	17	34	67	135
4	10	19	38	75	151
5	11	21	43	84	169
6	12	24	48	95	191

APPENDIX B

Characteristics of Kodak Panatomic-X SO-136 Film

TYPE SO-136
(June, 1966)

KODAK Special PANATOMIC-X Aerial Film, Type SO-136 (ESTAR Base)

Intermediate speed; high dimensional stability for mapping

BASE: 4-mil ESTAR polyester with dyed gel backing

SENSITIVITY: Panchromatic with extended red sensitivity

RMS GRANULARITY VALUE: 19 (Processed in KODAK Developer D-19 for 8 minutes at 68 F and read at a net density of 1.0)

RESOLVING POWER: 186 lines/mm at T.O.C. 1000:1 (D-19)
65 lines/mm at T.O.C. 1.6:1 (D-19)

SAFELIGHT: *Total darkness required.* A KODAK Safelight Filter, WRATTEN Series 3 (dark green), in a suitable safelight lamp with a 15-watt bulb can be used at not less than 4 feet for *only* a few seconds after development is half completed.

AERIAL EXPOSURE INDEX: Daylight—20
(Based on normal development of 8 minutes at 68 F in D-19)

FILTER FACTORS:

WRATTEN Filter	No. 12	No. 25
Factor	**2.0**	**4.0**

SPECTRAL SENSITIVITY
D-19
D = 1.0 above gross fog

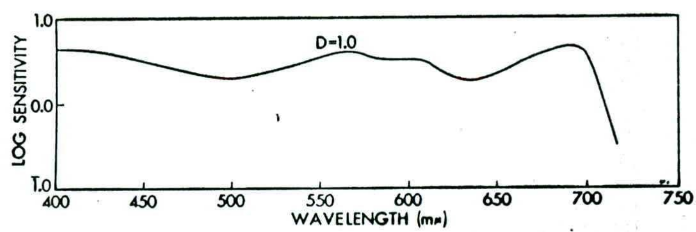

MODULATION TRANSFER CURVE

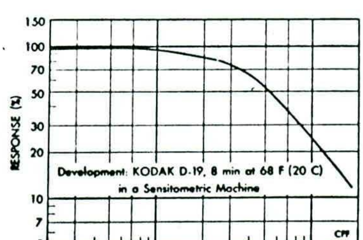

RECIPROCITY CHARACTERISTICS
D-19
D = 1.0 above gross fog

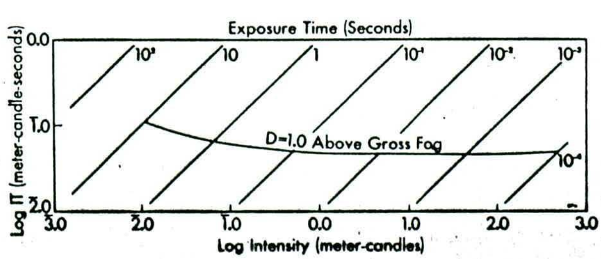

SENSITOMETRIC CURVES

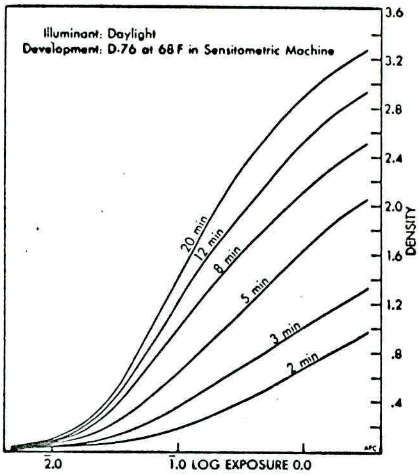

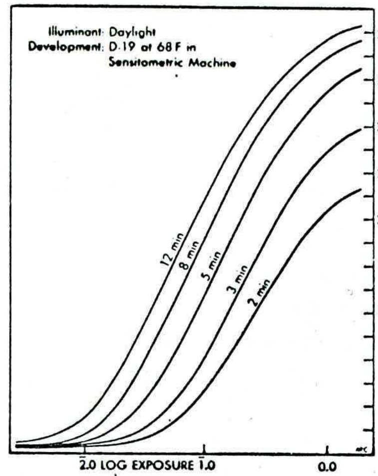

TIME-GAMMA CURVES
Illuminant: Daylight

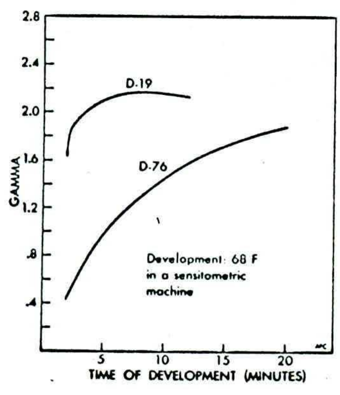

EASTMAN KODAK COMPANY • ROCHESTER, N. Y. 14650
Department GS
Section 19 — Data Sheets
6-66 Minor Revision
L-IPS-Bd
KODAK Publication No. M-118-N
PRINTED IN THE UNITED STATES OF AMERICA

APPENDIX C

Probability Calculations

The underlying objective of the external vibration phase of this study is to determine empirically what maximum image degradation could result from each applied test condition. While it would be desirable to take exposures at that instant of the vibration cycle when image velocity on the focal plane is the greatest, there is no practical means of achieving such precisely timed exposures. For this reason, the rules of probability theory are applied to indicate the approximate probability that at least one of many exposures is taken at a time when image motion will be near to its maximum value. For this experiment, it was determined that image motion, exceeding 90% of its maximum possible value during the period of the exposure, would be perfectly acceptable in determining empirically how much degradation could be expected. Therefore, in the following formulas, a successful event will be considered as an exposure being taken during which the image quality degradation recorded on film was the result of image motion which exceeded 90% of maximum image motion for the exposure time being used.

The probability formulas used herein are taken from page 42 of Cramer [9].

p = probability of a successful occurence of an event

q = probability of an event failure = 1 - p

n = the number of possible events, each having the same probability of success (p) and failure (q)

The probability of failure in all n events is equal to $q^n = (1-p)^n$.

The probability of success in at least 1 of n events = $1 - q^n$.

For a simple harmonic (sine wave type) of vibration with a single degree of freedom, the probability that the vibration at any instant is greater than 90% of peak velocity equals that percentage of time that the cosine function is greater than 0.9 in absolute value, which is about 28.7% of the time. Thus p in this case equals 0.287, and q equals 0.713. If n is taken as 20 exposures, then the probability of at least 1 of 20 exposures producing a successful event equals $1 - (0.713)^{20}$ equals 0.9988 or nearly 100%.

However, as was mentioned in Section II, the maximum torque in the XZ plane, which produces the maximum x-direction image motion, is caused when the Fx and Fz forces are both maximum in the same (clockwise or counterclockwise) direction about the center of gravity. Thus, the probability of near maximum torque is dependent on combined maximum conditions of two cosine functions simultaneously acting on the system.

The probability, for a single exposure, of both cosine functions exceeding 90% of maximum values in the same direction, equals (1/2 x .287) x (1/2 x .287) = 0.206 for a clockwise torque and 0.206 for a counterclockwise torque. In this case p = 0.0412, q = 0.9588, and the probability that 1 of 20 exposures will be successful equals $1 - (.9588)^{20}$ equals .56868 or about 57%.

This latter example would produce the probability percentage of interest if both Fx and Fz equally contributed to the degrading torque. Fortunately, this is not the case as Fx acts with a moment arm of about

130 mm, while Fz acts with a moment arm of about 17 mm (±7 mm depending on amount of film on spools). In the YZ plane, Fy acts with a moment arm of about 130 mm, while Fz acts with a moment arm of 10 mm. These moment arms (referred to as distances Dx, Dy and Dz in Section II) can be computed from the dimensions of Figure 1, assuming the elastic center to be at the geometric center of the three isolators.

While the exact probability determination would be computed by integrating a probability function with components of differing weights, an approximate solution is sufficient for this study.

One can consider the first example above to be a case where Fx acts on a Dz moment arm of 130 mm, while Fz acts on a Dx moment arm of zero. The probability of one of 20 events being sucdessful then equals 99.9%.

The second example above would be equivalent to both forces acting on moment arms of 130 mm; here, the probability of one of 20 events being successful equals 56.9%.

Although intermediate solutions would be non-linear, they can be approximated by linear interpolation between these two extremes. Using Dx = 17 mm, the probability of one exposure of 20 being successful equals 94.4%. Using Dy = 10 mm, the probability of one exposure of 20 being successful equals 96.7%.

In summation, the probability is about 94% that x-direction image degradation, for the poorest quality photograph of 20 taken under the same test condition, exceeds 90% of maximum possible image degradation for that test condition. Likewise, the probability is about 97% that the y-direction image degradation, for the poorest quality photograph of 20 taken under the same test condition, exceeds 90% of maximum possible image degradation for that test condition.

APPENDIX D

Resolution Prediction

For the stronger vibrations, where resolution degradation is in excess of 20%, Wernicke [10] found that resolution degrades quadratically in accordance with the formula

$$\frac{1}{R^2} = \frac{1}{R_s^{\,2}} + \frac{1}{S^2} \quad \text{where:}$$

R = degraded resolution value caused by vibrations, in lines/mm

R_s = static resolving power capability, in lines/mm

S = image motion during exposure, in mm

However, Wernicke did not study an aerial camera system, nor is there an easy way to measure how much image motion is obtained from vibration parameters normally known.

If one knew the angular rotation, made about the perspective center in either major direction from the principal axis of the lens, one could determine the maximum amount of image motion during any exposure. If θ is the single amplitude camera rotation angle (in radians) in any plane of interest, and the camera constant = 150 mm, then the image of a point on the principal axis would move back and forth from its central location with a single amplitude image motion of $A = 150 \text{ mm} \times \theta$ (since θ is quite small) or a total movement of 2A. However, an exposure which is quicker than the period of a low frequency vibration (which causes greatest image degradation) will only record a fraction of the total image motion. The product of vibration frequency and exposure time yields that fraction of the image motion cycle during which image motion is recorded. If that fraction of the total image motion cycle is called α, then maximum image motion is recorded when the exposure starts at $\alpha/2$ before the central position and ends $\alpha/2$ beyond that position.

For example, consider a camera with focal length of 150 mm, a shutter speed of 1/200th second, a vibration frequency of 5 cps which produces a single amplitude angular rotation of 0.00962 radians back and forth about the principal axis of the lens. $A = 150 \text{ mm} \times .00962 = 1.44$ mm; but image motion is recorded only during $1/200 \times 5 = 1/40$th of a cycle. $\alpha = 1/40 \times 360° = 9°$; $\alpha/2 = 4.5°$

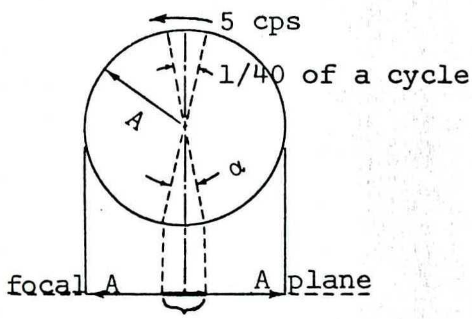

S = max image motion during 1/200 sec. exposure

Considering the maximum image motion as the projection of rotating vector A on the focal plane, the maximum image motion during a 1/200 second exposure:

$$S = (2)(A)(\sin \alpha/2)$$

$$= (2)(1.44)(\sin 4.5°) = .226 \text{ mm.}$$

The value of S found in this manner could then be inserted in the quadratic formula of Wernicke; however, the angle θ in the plane of interest is still an unknown.

Casper [5], nevertheless, provides an idealized method of obtaining the angle θ in any plane of interest, from parameters which are either known or can be computed or measured. Casper's approach will be listed below, with modifications to adjust his idealized method into a more general approach.

$\theta = T_d \times G_r$ where T_d is the disturbing torque due to displacement of the center of gravity from the elastic center of the isolators; and G_r is the isolator rotational transfer function. These terms are computed as follows:

$T_d = (a_c \cdot m \cdot d)$ where:

a_c = camera vibration acceleration = $a_f \times G_t$

a_f = external vibration acceleration

G_t = isolator translational transfer function

m = camera mass = camera weight/acceleration of gravity

d = moment arms of disturbing forces

In the diagram of section II, it can be seen that force Fx (caused by the camera mass multiplied by the camera acceleration in the x-direction) multiplied by the moment arm Dz produces a counterclockwise torque about the elastic center, as does the force Fz multiplied by moment arm Dx. At this point, all parameters would be known except G_t and G_r.

$$G_t = \frac{X_c}{X_f} = \frac{(2\zeta_t/\omega_{nt})f + 1}{(1/\omega_{nt})^2 f^2 + (2\zeta_r/\omega_{nr})f + 1}$$

$$G_r = \frac{\theta}{T_d} = \frac{1}{k_r[(1/\omega_{nr})^2 f^2 + (2\zeta_r/\omega_{nr})f + 1]}$$

X_c = double amplitude camera displacement (meters)

X_f = double amplitude external vibration displacement (meters)

θ = single amplitude camera rotation (radians)

T_d = disturbing torque (Kg/m)

L = effective spacing between isolators in plane of interest (meters)

ω_{nt}= natural frequency of isolator system in translation (rad/sec)

ω_{nr}= $L \cdot \omega_{nt}/0.5r$ (radians/second)

r = radius of gyration in direction of interest (meters)

k_t = translational spring constant of isolator (Kg/meter)

$k_r = 0.5 k_t L^2$ (Kg/meters)

ζ_t = damping factor of isolator system in translation (unitless)

$\zeta_r = 0.5\ L\zeta_t/r$ = damping factor of system in rotation (unitless)

m = camera mass ($\text{Kg}\cdot\text{sec}^2/\text{meter}$)

The external vibration displacement and frequency are the input vibration parameters for which image degradation is to be predicted. The various spacings should be known from the camera design diagrams.

The translational spring constants and damping factors of the isolators should be known from design data provided by the manufacturer. At a minimum, one would need a load-deflection diagram for the isolators, such as that shown at Figure 2. The spring constant is equal to the slope of the load-deflection curve at the point of loading. The individual isolator loads can be computed by moment analyses, as discussed in paragraph 3.4 of Beer and Johnston [11] or any Statics textbook. The damping factor is computed from isolator characteristic curve data as indicated in section VII of Pepi [12]. If these curves are not available- one could use a value of 0.2 and be fairly close to the value for the normal underdamped system. Errors in ζ have a very slight effect on the computed value of θ.

A moment analysis of the camera system used in this test was made. Considering a total weight of 90 Kg carried by the vibration isolators, with half a roll of film on either spool, the forward isolator carries a weight of 24.9 Kg, the left-rear isolator carries a weight of 34.9 Kg, and the right-rear isolator carries a weight of 30.2 Kg. The non-linear spring characteristics, and the unequal loadings, indicate that each spring has a different spring constant. From Figure 2.1, these spring constants are found to be approximately 9890, 24940 and 17270 Kg/meter, computed as the slope of the load-deflection curve at the weights carried by the isolators.

The characteristic curves of Figure 2.2 are for a 5 Kg loaded single degree of freedom system. Note the differences in the three curves. The vertical curve is smooth because the vertical movement is in the free direction. From Figure 2.1, it can be seen that the spring constant at 5 Kg is about 2040 Kg/meter. Since the natural frequency for a single degree of freedom system equals $\sqrt{k_t/m}$, the natural frequency in the vertical direction is found to be 63.2 radians/second or about 10.1 cps, as shown in Figure 2.2.

The lateral and longitudinal directions, however, have two natural frequencies. These are explained in section VII of Pepi [12]. Any attempt to restrict a system to a single degree of freedom is never fully achieved. Slight secondary degrees of freedom nearly always exist, which would allow slight movements in the longitudinal and lateral directions. Any direction in which an element of unbalance exists will have two resonant frequencies, from which natural frequencies are derived. The one lower in frequency is called the lower rocking mode, and the other is called the higher rocking mode.

Since most camera systems have 3 principal and 3 secondary degrees of freedom, there will be 3 lower and 3 higher rocking modes. The equations of motion for those modes are computed as indicated in chapter 3 of Tse, Morse and Hinkle [13]. If instrumentation is available a better method would be to determine the natural frequencies experimentally, as explained in section 2-11 by the same authors. Use only the 3 lower natural frequencies in the formulas by Casper if the isolators are stiff enough to strongly resist translational movement in the x and y directions and rotation about the z axis.

The radius of gyration in each direction is computed from $\sqrt{I/m}$, where I is the moment of inertia for the direction of interest, as computed by Beer and Johnston [11], page 321, or by numerous mathematics or engineering texts.

While this detailed analysis of resolution prediction might appear cumbersome, there is much to be learned from the equations, particularly for the purpose of camera design.

The major point to be observed is that vibrations would be no problem whatsoever if the center of gravity of the camera system were designed so as to be located very close to the elastic center of the isolators.

Even with current unbalanced systems, weights could be applied (similar to tire balancing weights on automobiles) to the camera so as to relocate the center of gravity closer to the elastic center.

Rocking motion of the camera system could be "broken up" by other simple methods, such as by steadying the camera with the hands of the camera operator.

Spacings between isolators should be the maximum practical within space limitations.

Vibration isolators should have low natural frequencies with strong damping factors.

Increased shutter speed is the best overall weapon against image motion.

Appendix E - Methods of Acutance Determinations

Figure E.1 - Normal Computational Method

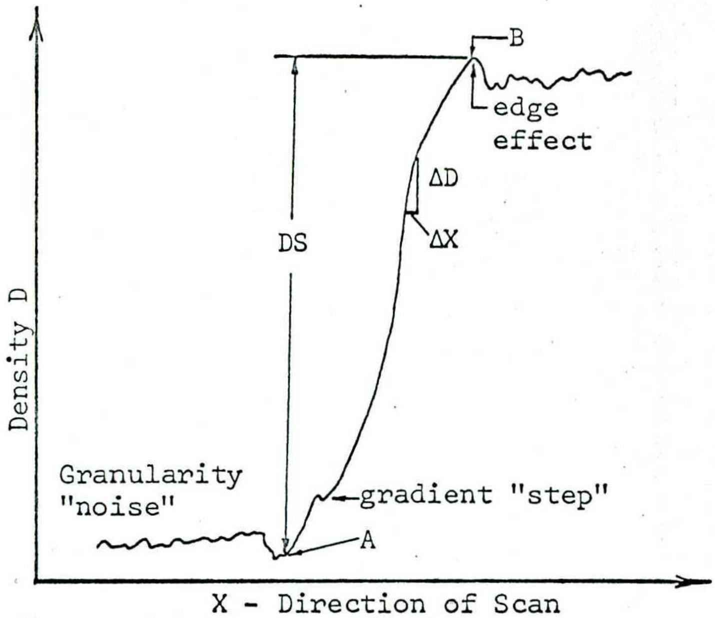

Acutance = $\bar{G}_x^2 / DS$ where:

DS is the density difference between points A and B along the curve where the gradient $\Delta D/\Delta X = .005$.

$$\bar{G}_x^2 = \frac{\Sigma(\Delta D/\Delta X)^2}{n}$$

which is the mean square of the gradient taken at n equal intervals of X between points A and B.

Figure E.2 - Lease Square Curve Fitting Method

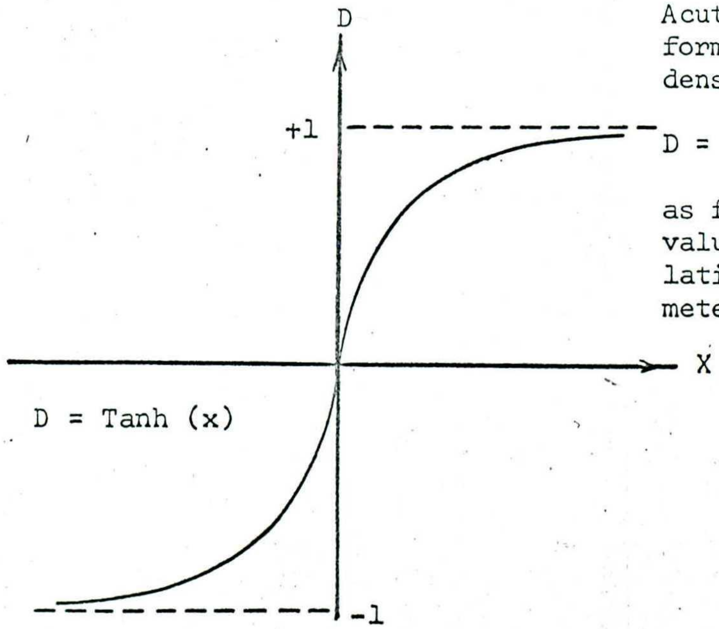

Acutance computed from same formula as above; however density values computed from

D = Hyperbolic tangent (X)

as fit to observed density values by the use of translational and scaling parameters in both directions.

The acutance of all edges was initially computed using the acutance formula expressed in Figure E.1 on the previous page. Unfortunately, it was difficult to decide where the points A and B occurred, because it was hard to distinguish gradient steps from granularity noise, both of which caused the gradient to be less than .005 and even negative. These factors had to be distinguished from each other because gradient steps are on the part of the curve over which the acutance is to be determined, while granularity noise is outside of the limits imposed by points A and B. Differing opinions as to where the cut-off points A and B occurred caused 30 - 40 % differences in acutance values.

In order to instill complete objectivity into the acutance determinations, a computer program was written to fit the density VS scanning distance data to an arctangent curve, which has the same general sigmoid shape. It was desired to obtain the parameters of the best fitting smooth curve through the procedures of least squares. One would then compute the acutance from the smooth curve where points A and B would be determined objectively.

In order to do this, it was necessary to translate the origin of the density (D) and scanning distance (X) data to the center of the sigmoid and then scale the data separately in the X and D directions. This was done by the method of observation equations initially, as explained on page 51 of Uotila [14]; with this procedure all four parameters (2 translational and 2 scaling) were considered as unknowns to be determined. Because of complications involving correlation of the scaling parameters, these two parameters were estimated and treated as weighted observations, and a combination observation/condition equation method was used, as explained on page 55 of Uotila [14]. Since there was no justification for estimating only 2 of the 4 parameters, all parameters were estimated, weighted and a least square adjustment was performed using the method of condition equations, as explained on page 53 of Uotila [14].

A variety of weighting techniques were used, but none of them produced a very good fit of a curve to the data. It was then decided to perform the procedure using the hyperbolic tangent curve. The hyperbolic tangent curve, shown in Figure E.2, has the same basic sigmoid shape, but would be more responsive to curve fitting techniques, because hyperbolic trigonometric functions are exponentially formed (reference page 224 of Selby [15]).

The hyperbolic tangent function, using the method of condition equations, provided the best fit of all procedures attempted. Most of the acutance values agreed, within about 25%, with the acutance values determined by the normal computational method. However, those scans with pronounced edge effects were found to produce a very poor fit to the data; furthermore, some of the acutance values by this method disagreed with the normal computational method values by more than 100%.

The fallacy of the whole curve fitting technique appears to be that the mathematical models used are not adequate representation of the data for which an artificial fit was desired. Since the edge effects belong on the traces, and should not be eliminated by artificial smoothing, there really is no reason why the data should fit the design curves of the mathematical models.

The curve fitting technique was abandoned, and a procedure was developed to objectively determine points A and B for use with the normal computational method of acutance determination. It was decided to mean the last 5 density values at either end of the scan so as to determine a leveled-off density value in the granularity noise area beyond the edge effects. Gradients less than .005 falling between these leveled-off density values were considered as gradient steps, and outside these values were considered as the points A and B. Thus, a quasi-objective technique of acutance determination was achieved.

BIBLIOGRAPHY

1. James, Thomas H. and Mees, Charles E., "Theory of the Photographic Process", Macmillan, 1966.

2. Fish, R. W., "Anti-Vibration Mountings for Aircraft Cameras," Photogrammetric Record, October 1958.

3. Crede, Charles E., "Shock and Vibration Concepts in Engineering Design", Prentice Hall, 1965, pp. 106 - 115.

4. Crafton, Paul A., "Shock and Vibration in Linear Systems," Harper and Brothers, 1961, pp. 160 - 198.

5. Casper, Richard, "Resolution of Vibration Isolated Cameras," Photogrammetric Engineering, July 1964.

6. Harris, Cyril M. and Crede, Charles E., "Shock and Vibration Handbook," Volume I, McGraw Hill, 1961.

7. Jones, L. A. and Higgins, G. C., Journal of the Society of Motion Picture and Television Engineers, Volume 58, 1952, pp. 277.

8. Higgins, G. C. and Wolfe, R. N., Journal of the Society of Motion Picture and Television Engineers, Volume 65, 1956, pp. 45.

9. Cramer, Harold, "The Elements of Probability Theory,", John Wiley and Sons, Inc., 1966.

10. Wernicke, Bruno K., "Effect of Image Motion on Resolving Power of a High-Acuity Lens-Film System," AD 240993, April 1960.

11. Beer, Ferdinand P. and Johnston, E. Russell Jr., "Mechanics for Engineers," McGraw-Hill Book Company, Inc., 1957.

12. Pepi, Jerome S., "Vibration Isolation of Optical Aerial Reconnaissance Sensors," Technical Report AFAL-TR-67-277, Oct. 1967.

13. Tse, Francis S., Morse, Ivan E. and Hinkle, Rolland T., "Mechanical Vibrations," Allyn and Bacon, Inc., 1966.

14. Uotila, Urho A., "Introduction to Adjustment Computations with Matrices," unpublished class notes, Department of Geodetic Science, The Ohio State University, 1967.

15. Selby, Samuel M., "Standard Mathematical Tables - 17th Edition," The Chemical Rubber Co., 1969.

16. "Vibrachoc-Caractéristiques de Construction et de Fonctionment des Supports Amortisseurs Entiérement Métalliques".